University of Naples “Federico II”

Ph.D. Program in Clinic and Experimental Medicine

XXIX cycle (2014-2017)

(Coordinator: Prof. Gianni Marone)

Prep1 deficiency affects olfactory system integrity by impairing TrkB-mediated neurotrophic signalling

Tutor:

Prof. Pietro Formisano

Ph.D. Candidate:

Dr. Serena Ricci

“Research is what I’m doing
when I don’t know what I’m doing”
(Wernher von Braun)

TABLE OF CONTENTS

LIST OF ABBREVIATIONS

A-P: anterior-posterior

Akt/PKB: protein kinase B

ANTP: antennapedia

BDNF: brain-derived neurotrophic factor

CB: cerebellum

CCL2: CC-chemokine ligand 2

CNS: central nervous system

COX: cytochrome C Oxidase

CX: cerebral cortex

DMB: diencephalic-mesencephalic boundary

E: embryonic stage

EPL: external plexiform layer

ERK: extracellular signal regulated kinase

FABP7: fatty acid-binding protein 7

FGF: fibroblast growth factor

GABA: gamma-aminobutyric acid

HAD: HIV-associated dementia

HIPP: hippocampus

HIV: human immune deficiency virus

HYP: hypothalamus

HOX: homeotic

HPF: hours post-fertilization

IGF1: insulin-like growth factor 1

IL: interleukin

MAPK: mitogen-activated protein kinase

MCP-1: monocyte chemoattractant protein 1

MHB: midbrain-hindbrain boundary

M/T: mitral/tufted

N2A: neuro2A

NGF: nerve growth factor

NSC: neural stem cells

NT-3: neurotrophin-3

NT-4/5: neurotrophin-4/5

OB(s): olfactory bulb(s)

OSNs: olfactory sensory neurons

OXPHOS: oxidative phosphorylation

Pax6: paired box 6

Pbx1: pre-B cell leukemia transcription factor

PDX1: pancreatic and duodenal homeobox factor 1

PG: paralogue group

PGCs: periglomerular cells

PM: Pbx-Meis binding site

Prep1: Pbx regulating protein 1

r: rhombomere

RMS: rostral migratory stream

SNP: single nucleotide polymorphism

SVZ: subventricular zone

TALE: three-amino acid loop extension

TNFR(s): tumour necrosis factor receptor(s)

Trk(s): tropomyosin receptor kinase(s)

UEF-3: urokinase enhancer factor-3

uPA: urokinase plasminogen activator

Vps10p: vacuolar protein sorting 10 protein

Wnt: wingless integration site

ABSTRACT

Prep1 is a transcription factor belonging to the TALE proteins, which plays an important role in the embryonic development of the hindbrain. However, as reported on web-based atlas, morphological data revealed that Prep1 expression is kept also in adult mouse brain and, in particular, within the olfactory bulb (OB), even though its function is still unknown. In order to investigate the role of Prep1 in olfactory nuclei I used a *prep1* hypomorphic mouse (*prep1*$^{i/+}$), which express about 55-57% of protein. Brain morphological analysis revealed that *prep1*$^{i/+}$ mice feature a significant reduction of OB area, a reduced number of periglomerular interneurons and an increased number of mitral cells within the main olfactory bulb, compared to WT mice. *prep1*$^{i/+}$ mice OB cytochrome C oxidase staining showed also a reduced neuronal metabolism within the glomerular layer. Consistently, olfactory perception test highlighted that hypomorphic mice display a low ability to distinguish odor scents, accompanied to a significant locomotor hypoactivity. Molecular analysis, indeed, revealed that *prep1*$^{i/+}$ mouse olfactory nuclei express reduced levels of TrkB, the downstream receptor of BDNF, the main neurotrophic factor involved in olfactory plasticity and functions. In parallel, also a decreased activation of molecular mediators involved in TrkB-mediated neurotrophic signalling (Akt, ERK) was observed. Congruously, mouse neuronal cells (N2A) overexpressing Prep1 showed increased cell growth, viability and metabolism, with high levels of TrkB expression and Akt/ERK phosphorylation, compared to control cells. Thus, our data suggest that Prep1 deficiency alters olfactory system morpho-functional integrity by affecting TrkB expression and signalling pathway, giving a rationale to further investigate Prep1 as potential marker in olfactory dysfunctions associated to impaired responsiveness to BDNF signalling.

1. BACKGROUND

1.1 Central Nervous System (CNS): comparative anatomy, functions and development in rodents and human

The central nervous system (brain and spinal cord) controls the rest of the body via the peripheral somatic (sensorimotor or voluntary) and autonomic (involuntary) nervous systems, by functional domains based on contiguous signalling pathways. Relative to other organs and body systems, the elements of the normal CNS are anatomically different within and among species, exhibiting major structural changes at both gross and microscopic levels. Neuroanatomic comparison between mice and human brain underlined a marked difference in size and organization, as well as in the functional and structural arrangements (Figure 1). For example, whilst human brain has great size (approximately 1300 gr) with a lobular organization, the mouse brain is quite small (~0.4 g) and not prominently lobed, with a pale colour due to its high lipid content. Another pronounced divergence is that mouse brain is lissencephalic (does not have sulci or gyri). Nevertheless, although mouse and human brain vary somewhat in the organization and size of various brain regions, they are comparable with respect to specific anatomic pathways, functions, and relationships therein. Many mouse neuroanatomic structures, in fact, are comparable to human brain regions involved in neurological disorders, such as the cerebral cortex in Alzheimer's disease, the striatum in Huntington's disease or substantia nigra in Parkinson's disease. For these reasons, mouse brain can represent a good model for the study of functional and morphologic alterations of human diseases.

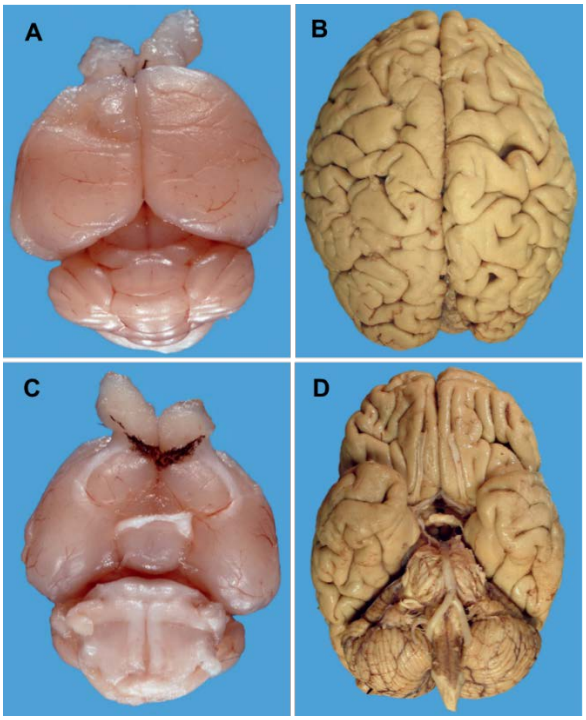

Figure 1: Major gross features of the dorsal (A and B) and ventral (C and D) surfaces of fixed brains from an adult C57BL/6 mouse (A and C) and human (B and D). Figure adapted from Hagan CE, Bolon B, Keene CD. Nervous System (chapter 20); "Comparative Anatomy and Histology" Edited by: Treuting PM, Dintzis S, Liggitt D and Frevert CW. Elsevier Inc. 2012, ISBN: 978-0-12-381361-9

The most extensive brain regions are the cerebral cortex, which is prevalently composed of granule and pyramidal neurons, and the basal ganglia, which includes the striatum (caudate nucleus and putamen), globus pallidus, subthalamic nucleus, and substantia nigra. In the human brain, the caudate nucleus and putamen are separate but semi-continuous structures in the striatum, while in mice the striatum is a single structure and is the most extensive of the basal nuclei. The hippocampus is part of the limbic system, which includes the amygdala, fornix, habenular nuclei, hippocampus, hypothalamus, septum, and anterior thalamic nucleus. In both species, the limbic system regulates emotions and behaviours that are important to socialization, survival (feeding, fighting, and fleeing) and memory. The thalamus is a structure that underscores how

understanding the connectivity between brain regions and can facilitate localization and identification of lesions. The thalamus forms the central part of the diencephalon and is the seat for multiple nuclei that relay sensory information between lower brain centres and the cerebral cortex. The hypothalamus, which lies ventral to the thalamus, integrates the homeostatic functions of the autonomic, endocrine, and somatosensory systems. Numerous behaviours are regulated by this area, including those involved in cardiovascular tone, ingestion (eating and drinking), parental care, self-preservation, sex, and thermoregulation. The basic anatomic relationships and pathways in the thalamus and hypothalamus are conserved between rodents and human. Finally, the cerebellum has a grey matter cortical layer and a central white matter core. It is naturally divided into distinct lobes which do not correlate exactly to the functional divisions and its histologic structure is also remarkably conserved between rodents and human.

At cellular level, CNS can be divided into two categories based on their embryonic origin. Cells arising from the neuroectodermal layer include neurons, astrocytes, oligodendrocytes, and ependymal cells. Cells of mesenchymal origin include the meninges, blood vessels, and microglia. The neuron represents the functional unit of the nervous system which receives input from other neurons or non-neural tissues, such as the musculature. Neurons can be categorized on the basis of their neurotransmitter phenotype (e.g. GABAergic, cholinergic, serotoninergic, etc.), their morphologic appearance (e.g. pyramidal, granule, etc.) and the number of processes extending from the cell body (e.g. uni-, bi-, multipolar). Neurons have a high metabolic rate, which makes them extremely vulnerable to certain global toxic insults that impair intracellular energy metabolism (Hagan CE *et al.*, 2012)

Concerning brain organogenesis, the first major event in CNS development of all vertebrates is the formation of a specialized fold of ectodermal tissue called the neural tube, from which the spinal cord and brain subsequently differentiate.

Neural tube formation occurs approximately at mid-gestation in rodents, while in human, this event occurs earlier during prenatal development. The anterior portion of neural tube generates three primary vesicles: forebrain (prosencephalon), midbrain (mesencephalon), and hindbrain (rhombencephalon) (Figure 2). The prosencephalon becomes subdivided into the telencephalon, which will form the cerebral hemispheres, and the diencephalon, which will form the thalamic and hypothalamic brain regions. The mesencephalon does not become subdivided, and its lumen eventually becomes the cerebral aqueduct. The rhombencephalon becomes subdivided into the myelencephalon, which becomes the medulla oblongata, whose neurons generate the nerves that regulate respiratory, gastrointestinal, and cardiovascular movements, and the metencephalon, which gives rise to the cerebellum, the part of the brain responsible for coordinating movements, posture, and balance. Periodic swellings, called rhombomeres, divide the rhombencephalon into smaller compartments that represent separate developmental "territories" where the cells can mix freely with each other but not with cells from adjacent rhombomeres (Rice D and Barone S, 2000; Gilbert SF, 2000).

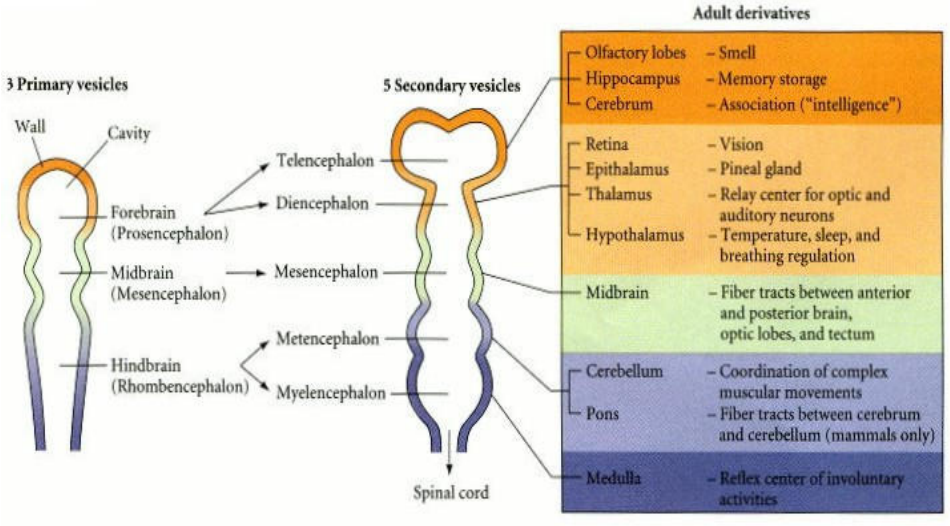

Figure 2: The three primary brain vesicles in early brain development. Figure adapted from Gilbert SF. Developmental Biology. 6th edition. Sunderland (MA): Sinauer Associates; 2000. Differentiation of the Neural Tube.

Numerous genes, including transcription factors, signalling molecules, membrane and nuclear receptors, are expressed in segmental manner during brain development and most of these genes explain dynamic patterns of activity.

1.2 Molecular regulators of CNS development

1.2.1 Neurotrophins

Neurotrophins belong to the class of growth factors and include nerve growth factor (NGF), brain-derived neurotrophic factor (BDNF), neurotrophin-3 (NT-3) and neurotrophin-4/5 (NT-4/5), which are all widely recognized as essential factors in the developing central nervous system. Structure of all neurotrophins is highly conserved among species and is characterized by a six-cysteine residues motif that enable formation of disulphide bridges. Neurotrophins are synthesized as pre-proproteins by both neuronal and non-neuronal cell types. When the hydrophobic region at the N-terminal of the signal peptide is removed from pre-proneurotrophin, the proneurotrophin is generated. The proneurotrophin is either cleaved of the signal peptide in the endoplasmic reticulum and converted to the mature neurotrophin. Mature neurotrophins are secreted as homodimeric proteins into the extracellular space and act in a paracrine and/or autocrine way, controlling many crucial processes in CNS development, such as proliferation, migration, differentiation, survival, apoptosis and synaptic plasticity. These effects are mediated by the interaction with three distinct classes of receptors: 1) three members of the tropomyosin receptor kinase (Trk) family (TrkA, TrkB and TrkC), which mediate neurotrophic effects via Ras/MAPK and PI3K/Akt signalling pathways; 2) the low-affinity p75 neurotrophin receptor ($p75^{NTR}$) belonging to the tumour necrosis factor receptor (TNFR) superfamily; 3) sortilin, a Vps10p domain-containing transmembrane protein (Figure 4). All neurotrophins mediate their effects via activation of one or more Trk receptors, with a different binding

affinity. At the same time, Trk(s) are able to bind other neurotrophic factors, such as Insulin-like growth factor (IGF1) which, through a feedback mechanism, might control their expression (Li H *et al.*, 2013). There is a high affinity between TrkA and NGF, and both NGF/TrkA and NGF/$p75^{NTR}$ complexes control neuronal survival, differentiation, and the level of innervation during the development of the central and peripheral nervous system. TrkB has the highest binding affinity to BDNF and NT-4, which play important roles in the survival and function of neurons of all CNS but particularly within hippocampus and cortex. TrkC has been reported to be activated almost exclusively by binding to NT-3 and it regulate viability and differentiation of sensory neurons. Unlike the Trk receptors which auto-phosphorylate after ligand engagement, the $p75^{NTR}$ does not have intrinsic catalytic activity. Instead, it partners with the Trk receptors and, by increasing the affinity of the mature neurotrophins, supports pro-survival and pro-growth signalling. In contrast, when it binds no-Trk receptor, such as sortilin, it generally activates the apoptotic pathways and death processes, which equally are essential to the development, maturation and maintenance of the nervous system (Reichardt LF, 2006; Stoleru B *et al.*, 2013; Bothwell M, 2016).

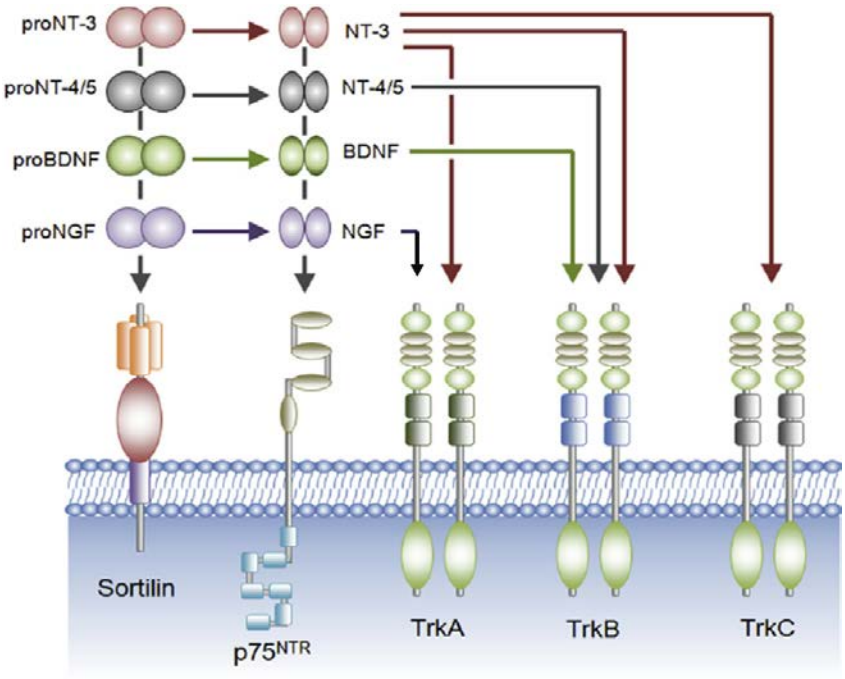

Figure 3: Schematic design of neurotrophic receptors and their ligands. Figure adapted from Bradshaw RA, Pundavela J, Biarc J, Chalkley RJ, Burlingame AL, Hondermarck H. NGF and ProNGF: Regulation of neuronal and neoplastic responses through receptor signaling. Adv Biol Regul. 2015; 58:16-27.

During mammalian CNS formation, neurotrophins expression levels are selectively different with respect to developmental stages and to various structures of the nervous system. NGF and its TrkA receptor are expressed prevalently during mid-stages of development (the 15-16th week of gestation in human). However, in mouse, expression of TrkA receptor also occurs at early stages of brain development, with the highest density within the sensory cranial and spinal dorsal root ganglia, where it regulates embryonic sensory neurons survival. NGF knockout mouse pups (*ngf*$^{-/-}$), in fact, have a short life span, due to the massive cell loss in the sensory and sympathetic ganglia. In the same way, TrkA null mice display significantly fewer and smaller cholinergic neurons in the basal forebrain and striatum, and die shortly after birth, indicating that the NGF/TrkA signalling plays an important role in maturation of neurons.

Expression of BDNF, NT-4/5 and TrkB receptors also occurs at early

stages of development of the mammalian nervous system especially within the trigeminal ganglia. Beginning from E13, BDNF is also present in the developing cortical plate neuroblasts of the rat. BDNF knockout mice feature poor motor coordination and body balance and die before the second postnatal week. In mouse, TrkB expression is visible at E9.5 in the neuroepithelium and neural crest cells that form the dorsal root ganglia and, then (E13.5), within the lateral wall of the telencephalon, trigeminal nerve and the sensory ganglia of the spinal cord. At E16.5 particularly, high levels of TrkB expression in the CNS are visible in the olfactory lobe and ependymal layer of the fourth ventricle. TrkB knockout mice (*trkB* $^{-/-}$) display abnormalities in the facial motor nucleus and trigeminal ganglion and die within 48h after birth.

Pattern distribution of NT-3 and its TrkC receptor during rodents development has been also accurately investigated. In the early stages of neural tube formation, NT-3 expression has been observed in the ventricular zone cells and primordial plexiform layer, as well as TrkC expression which, in mid-stages, is visible also in the neocortex, striatum, pons, medulla, cerebellum and the mantle (post-mitotic) layer of the spinal cord. NT-3 deficient mice display severe loss of the cranial and spinal sensory and sympathetic neurons and most of them die shortly after birth, while mice lacking TrkC show reduced numbers of sensory neurons and glial cells, displaying behaviour impairments.

Expression of $p75^{NTR}$ in rat has been observed at early developmental stages of the CNS, particularly in the forming dorsal root and sensory ganglia. From E13, its expression increase during following days. Mice lacking $p75^{NTR}$ display behavioural impairment and loss of neurons in the basal forebrain. Sortilin receptor was observed to be strongly expressed in the late stage of brain development, especially within the cerebral cortex and retina. Sortilin knockout mice, in fact, feature reduced neuronal apoptosis (Huang EJ and Reichardt LF, 2001; Bartkowska K *et al.*, 2010).

1.2.2 HOX proteins

The *Hox* genes family, originally discovered in segmental identity processes along the anterior-posterior (A-P) axis of *drosophila melanogaster*, encompasses a set of developmentally regulated transcription factors characterized by the presence of a 180-nucleotide sequence called “homeobox” encoding a 60-aminoacid DNA binding motif known as the “homeodomain”. Many HOX factors regulate gene expression during developmental patterning or cell differentiation, thus, mutations in these genes can cause dramatic changes to developmental programs in a wide range of organisms, including human. *Hox* genes belong to the Antennapedia (ANTP) class, which includes the closely related *Parahox* genes, *NK* genes, and various others. The number of functional homeobox genes increases in the vertebrate lineage with duplications of the original homeotic complex which generate four different *Hox* genes complexes in mammals (A, B, C, and D) (Figure 3). Because the different complexes are the result of duplications, *Hox* genes with the same rank in different complexes are evolutionary relatives and are therefore called “paralogues” (Trainor PA *et al.*, 2000; Holland PW and Takahashi T, 2005; Hrycaj SM and Wellik DM, 2016).

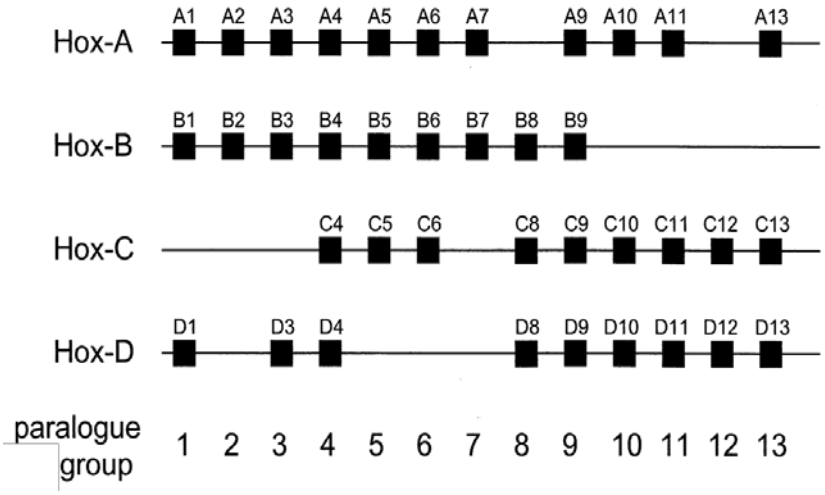

Figure 4: Genomic organization of *hox* genes clusters in mammals. Figure adapted from Glover JC. Correlated patterns of neuron differentiation and *hox* gene expression in the hindbrain: a comparative analysis. Brain Res Bull. 2001; 55:683-693

HOX proteins are known to play important roles in specifying the regional identity and pattern of neuronal differentiation within the hindbrain. *Hox* genes expression is established at early neural plate stages (E7.5-8.0 in mouse), before the formation of definitive rhombomeres (r), and it is enhanced by retinoic acid or fibroblast growth factor (FGF). HOX expression is dynamic during the period of rhombomeres segmentation, and is maintained up to late stages of hindbrain development well after morphological segmentation has disappeared (Glover JC, 2001).

Functional support for the role of *Hox* genes in regulating the segmental identity of hindbrain rhombomeres has come through analyses of phenotypes arising from loss- and gain-of-function experiments in several species. The gene products of the paralogues group 1 (PG1), *Hoxa1* and *Hoxb1*, play multiple roles in mouse hindbrain, which, in part reflect their regulatory relationship, because *Hoxa1* helps to activate *Hoxb1* in r4. Moreover, *Hoxa1* has an additional role in forming r5. Indeed, *Hoxa1/Hoxb1* mutants fail to adopt a segmental identity, and no neural crest cells migrate from r4 segment. *Hoxa2* is the only PG2 member expressed in r2 and it is required to maintain r2 segmental properties. Several evidences from other species indicate that *Hoxa2* plays a conserved role in regulating the differentiation of bone and connective tissue in craniofacial development. *Hoxa2* and *Hoxb2* are both expressed also in r3-r7 segments. In mouse, analyses of single and compound mutants for these genes showed that *Hoxa2* influences the size of r3, and *Hoxb2* contributes to the maintenance of r4 identity. The PG3 gene products, *Hoxa3*, *Hoxb3* and *Hoxd3*, work in concert to regulate the identity of r5 and r6 in part through repression of *Hoxb1*. Finally, the PG4 genes *Hoxa4*, *Hoxb4*, and *Hoxd4* are expressed up to the r6/r7 border and mutants display severe skeletal abnormalities. However, no hindbrain or neurological defects have been reported even in compound mutants in which all three of these PG4 genes are deleted (Alexander T *et al*., 2009).

In the late stages of hindbrain development, HOX proteins are able to

transform uniform segments into remarkably elaborate structures. The segmented expression of *Hox* genes in the hindbrain, in fact, will reflect the organization of neural crest cells. The even-numbered rhombomeres and r1 will generate the vast majority of hindbrain crest cells, which will migrate ventrally in three distinct streams at the axial levels and will populate the pharyngeal arches giving rise to cranial sensory ganglia and mesenchyme, and contributing to the formation of skeletal and vascular structures (Rijli FM *et al.*, 1998).

1.2.3 TALE proteins

The three-amino acids loop extension (TALE) homeodomain proteins are recognized as transcription factors responsible for regulating growth and differentiation during vertebrate embryogenesis. The genes encoding these proteins are highly conserved and are present in the common ancestor of plants, fungi, and animals. TALE proteins display a highly conserved DNA binding domain of approximately 60 amino acids called the homeodomain. This region is composed of three alpha helices and a flexible N-terminal arm. The homeodomain interacts with the DNA through the third helix making base-specific contacts in the major groove of DNA and through the N-terminal arm which contacts the minor groove of DNA. Between the first and the second alpha helices of the homeodomain there is an extension of three amino acids, virtually represented by a proline (P) – tyrosine (Y) – proline (P) in position 24-26. This domain has been implicated in protein–protein interactions that are required for fundamental aspects of development.

The TALE homeodomain superclass is composed of two groups: the PBC and the MEIS families. The PBC subclass, referring to the conserved PBC motif N-terminal to the TALE homeodomain, includes the vertebrate Pbx proteins, fly Extradenticle and worm Ceh-20. The MEIS class includes Homothorax (Hth) in flies and the Meis and Prep proteins in vertebrates (Figure

5). Cooperative function among TALE family members is critical for transcription regulation during the developmental programs (Moens CB and Selleri L, 2006; Longobardi E *et al*., 2014).

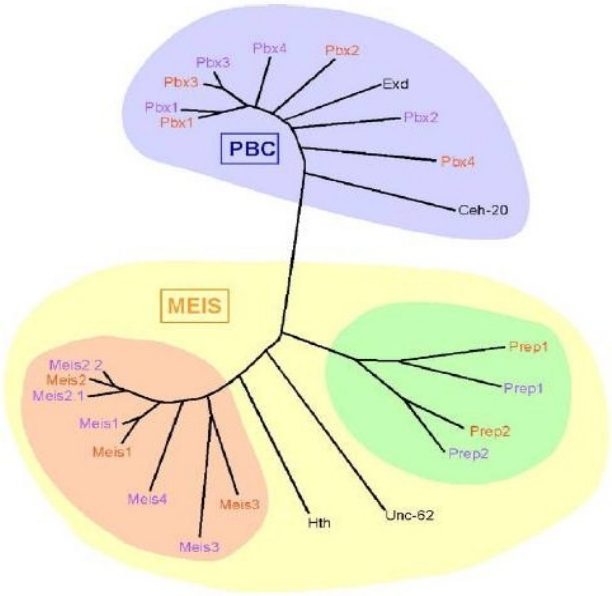

Figure 5: Phylogeny of TALE proteins. TALE homeodomain proteins are divided into two groups: the PBC family, including the vertebrate Pbx proteins, fly Extradenticle and worm Ceh-20, and the MEIS family, including vertebrate Meis and Prep proteins, fly Homothorax (Hth) and worm Unc-62. Orange letters indicate mouse proteins and purple letters indicates their zebrafish orthologues.

A wide body of literature have underlined the irreplaceable involvement of TALE proteins in the early and late stages of CNS development, with different implication related to the brain vesicles they are expressed in. The most studied role of TALEs has been in the cooperation with HOX family transcription factors in defining hindbrain rhombomeric identities along the A-P axis. Experimental observations in zebrafish and *xenopus laevi* support a model for initial hindbrain induction, in which mesodermal Wnt3a signaling initially acts upstream to Meis3/Pbx proteins, which, subsequently, induce PG1 HOX(s) and FGF3/8 expression in r4, activating segmentation of the hindbrain into distinct rhombomeres. Indeed, Meis3 null zebrafish embryos showed no-proper

hindbrain formation. Meis, Pbx and HOX proteins interact at two distinct levels. Early in development, Meis proteins activate PG1–4 *Hox* genes expression in the hindbrain and then, Meis/Pbx/HOX protein complexes bind target genes (also *Hox* genes themselves) to activate their transcription. For example, in mouse, HOXA1 together with Meis/Pbx proteins activate the *hoxb1* gene enhancer, and later, HOXB1, together with HOXB2, Meis3, and Pbx2/4 proteins promote maintenance of Meis/Pbx expression in r4 (Schulte D and Frank D, 2014).

Studies on transgenic models observed the involvement of PBX and MEIS proteins also during the development of the midbrain, which is an important center of sensory-motor integration. In zebrafish, PBX proteins cooperate with homeodomain transcription factor Engrailed to compartmentalize the midbrain by regulating the maintenance of the midbrain-hindbrain boundary (MHB) and the diencephalic-mesencephalic boundary (DMB). Indeed, zebrafish embryos lacking PBX, display an impaired development of mesencephalic region of the neural tube (Erickson T *et al.*, 2007). In mouse, Meis2 and Pbx2, are specifically expressed in the entire region of the dorsal mesencephalon, where they synergistically regulate transcription of EphA8 receptor involved in the proper development of retinotectal projection (Shim S *et al.*, 2007). In the ventral midbrain development, recent studies implicates PBX proteins in dopaminergic cell differentiation. Indeed, Pbx1 deficient mice display a misrouted dopaminergic neurons axon projections (Sgadò P *et al.*, 2012).

TALEs have also been investigated in the regulation of several steps of forebrain development. In mouse, Meis1 and Meis2 expression has observed to be high in the ventrolateral telencephalon, which represents the major source for GABAergic interneurons of the cerebral cortex, hippocampus, and olfactory bulb (Toresson H *et al.*, 2000; Parnavelas JG, 2000). Meis1 expression is induced during forebrain-derived neural stem cells (NSC) differentiation in the absence of *Hox* genes, and is expressed in both cortical neurons and astrocytes

(Barber BA *et al.*, 2013), while Meis2 seems to be critical during cranial neural crest cells development, as Meis2 deficient mouse embryos display defects in neural crest-derived tissues and abnormal cranial nerves (Manchon O *et al.*, 2015).

1.2.3.1 Prep1

Prep1/Pknox1 (PBX regulating protein 1) is a 64 kDa ubiquitary homeodomain transcription factor belonging to the MEIS subclass of the TALE family proteins, mapping on the chromosome 21q.22.3. The Prep1 homeodomain is structurally related to the PBC homeodomain class and contains an isoleucine residue in the third position of the conserved WF_N sequence in the homeodomain. Indeed, Prep1 forms DNA-independent dimeric complexes with the Pbx1 homeodomain transcription factors, enhancing its target specificity and regulatory function. Prep1 shares homology with MEIS proteins within the homeodomain and in two well-preserved homology amino terminal regions, termed HM1 and HM2, which bind the N-terminal region of Pbx1 (PBC-A) and are essential for Prep1-Pbx1 heterodimerization, which in turn is required for DNA binding. Prep1 could be localized both in cytoplasm and in nucleus and the heterodimerization with Pbx1 appears to be essential for translocation of Prep1 into the nucleus and DNA target binding. In addition, Prep1 dimerization prevents nuclear export and the proteasome degradation of Pbx1, prolonging its half-life. Formation of dimeric complex drastically increases binding affinity of Prep1/Pbx1 to the DNA. Together Prep1 and Pbx1 form the UEF-3 (Urokinase Enhancer Factor-3) transcription factor. The UEF-3 DNA target site is a regulatory element present in the promoters of several growth factors, proteases and inflammatory mediators genes, such as interleukin-3 (IL-3), stromelysin and urokinase plasminogen activator (uPA). Prep1 and Pbx1 can form ternary complexes with PDX1 to regulate somatostatin gene transcription (Longobardi E *et al.*, 2014)

The role of Prep1 has been in part clarified by the generation of mutant mice. Nevertheless, Prep1 null mouse embryos results in early lethality before gastrulation (E7.5) (Fernandez-Diaz LC *et al.*, 2010), precluding a study of the Prep1 role in later developmental processes. An insertion of a retroviral vector in the first intron of the *prep1* gene results in a homozygous (*prep1*$^{i/i}$) or heterozygous (*prep1*$^{i/+}$) hypomorphic mutation that exhibits variable penetrance and expressivity. *prep* $^{i/i}$ mouse embryos die between E17.5 and P0 and present a profound alteration in the hematopoietic development and profound anemia (Ferretti E *et al.*, 2006). However, a small percentage of them are born alive and subsequently live a normal length-life, showing T-cell development anomalies with a decreased number of circulating $CD4^+$ and $CD8^+$ T cells and increased apoptosis (Penkov D *et al.*, 2005). In addition, *prep1*$^{i/i}$ mice feature an impairment of erythropoiesis and angiogenesis accompanied by liver hypoplasia, decreased hematocrit, anemia, and delayed erythroid differentiation, with a decrease in capillary formation (Ferretti E *et al.*, 2006). These mice show also alterations in eye development and a reduced lens size, similar to the phenotype of Pax6 deficient mice. Prep1 deficiency affects the expression of both TALE class partners Pbx1 and Meis proteins, both required for embryonic hematopoiesis (Azcoitia V *et al.*, 2005; DiMartino JF *et al.*, 2001; Hisa T *et al.*, 2004). In addition, our laboratory has recently evidenced an important role of Prep1 in glucose homeostasis, regulation of insulin-action in muscle and liver, and in the regulation of hepatic lipogenesis (Oriente F *et al.*, 2008; Oriente F *et al.*, 2011; Oriente F *et al.*, 2013).

Several *in vivo* observations have underlined a key homeotic role of Prep1 in early stages of brain development. *In situ* hybridization analysis on zebrafish embryos showed that *prep1* gene is ubiquitously expressed up to 24 hours post-fertilization (HPF) and restricted to the head from 48 HPF onwards where it is critically involved in apoptosis and differentiation processes during neuronal crest cell differentiation and in craniofacial chondrogenesis (Deflorian G *et al.*, 2004). It has been demonstrated that, during zebrafish embryogenesis,

the formation of Prep1-Pbx1-Hoxb1/2 trimeric complex, through the Pbx-Meis binding (PM) site, represents an essential support for Hoxb(s) in segmentation of r3 and r4 rhombomeres (Choe SK *et al.*, 2002). Studies performed on mouse embryos also confirmed that Prep1 is deeply expressed in hindbrain since day 9.5 and that it confers high stability to Prep1-Pbx1-Hoxb1 multimeric complex in r4 rhombomere development (Jacobs Y *et al.*, 1999; Ferretti E *et al.*, 2000; Ferretti E *et al.*, 2005). In human, very little is known about the role of Prep1 in CNS embryonic development, as well as in adult cerebral functions. Analysis of fetal half-brain diagnosed as trisomic for chromosome 21 (Down Syndrome) revealed that *prep1* gene overexpression is related to an increased expression of FABP7 (Fatty acid-binding protein 7) which is strongly related to impaired glio- and cortical neurogenesis that can partially explain the early neurological impairments occurring in these subjects (Sánchez-Font *et al.*, 2003). In contrast, some years later, Pereira PL observed that in a mouse model of Down Syndrome (Ts1Yah mouse) the hippocampal overexpression of Prep1 may facilitate learning and memory (Pereira PL *et al*., 2009). One observational study on HIV (Human Immune Deficiency Virus) patients showed that a single nucleotide polymorphism (SNP) rs2839619 in *prep1* gene is significantly associated to an increased expression of chemokine MCP-1 which is strongly implicated in HIV-Associated Dementia (HAD) (Bol SM *et al.*, 2012). The involvement of Prep1 in HAD has been also indirectly related to the presence of a -2578G polymorphism in CCL2 promoter which increases Prep1 binding and favours the overexpression of this brain pro-inflammatory mediator (Wright EK *et al.*, 2008).

2. AIM OF THE STUDY

The complex anatomy and functions of the Central Nervous System (CNS) arise from the requirement to support multiple sensory and structural activities by the different brain components, which during embryonic development are generated independently and subsequently united, achieving a level of structural integrity. These processes are under the tight control of several molecular mediators, such as the neurotrophins and, in particular, the homeobox proteins which are involved not only in all neurogenesis steps but also in sustaining and promoting neuronal growth and sensory-motor functions from post-natal to maturity age. The combination of previous *in vitro* and *in vivo* studies, which characterized basic mechanisms and functions of these factors, has proven instrumental for understanding the associated developmental defects, as well as adulthood neuronal diseases. Prep1/Pknox1 is one of the most recently discovered homeobox factors, which has a pivotal role in rodents during rhombencephalon segmentation and actively participate to many processes for midbrain and forebrain genesis. However, no evidence has defined the impact of this transcription factor in normal adult mouse CNS functions and whether changing in Prep1 expression might be implicated in neurological impairments observed in many neurodegenerative and behavioural disorders. The aim of my study has been to investigate the implication of Prep1 in the correct morphogenesis and function of adult mouse brain and, by using a *prep1* hypomorphic mouse model, I purposed to evaluate whether the deficiency of this gene might affect nervous system integrity and behaviour. In addition, by using a more standardized *in vitro* neuronal system, I analysed the main molecular mechanism by which Prep1 exerts its effect on neuronal cell functions.

3. MATERIALS AND METHODS

3.1 Materials

Media, sera, antibiotics for cell culture and the lipofectamine reagent were from Invitrogen (Grand Island, NY). The Prep1, Actin, $p75^{NTR}$, TrkB, IGF1Rβ, p-AKT1/2/3(Ser473), AKT1/2, ERK1/2, IκBα, 14-3-3θ antibodies were from Santa Cruz Biotechnology, Inc. (Santa Cruz, CA). The p-ERK1/2(Thr202/Tyr204) and p-IκBα(Ser32/36) antibodies were from Cell Signaling Technology, Inc. (Danvers, MA). Protein electrophoresis and Real Time PCR reagents were purchased from Bio-Rad (Hercules, CA), Western blotting and ECL reagents from Amersham Biosciences (Arlington Heights, IL). Mayer Hemalum staining was from Bio-Optica S.p.A (Milan, IT). Tissue-Tek OCT was from Sakura Finetek Usa, Inc. (Torrance, CA). Cytochrome C, Bovine Catalase, DAB, Sulforhodamine B, Eukitt and all other chemicals was from Sigma-Aldrich (St. Louis, MO).

3.2 C57BL/6J *prep1* hypomorphic mice

C57BL/6J *prep1* targeted mice were generated by gene-trapping by Lexikon Genetics, Inc. (The Woodlands, Texas) and have been previously described (Ferretti E *et al.,* 2006; Penkov *et al.,* 2005; Fernandez-Diaz *et al*., 2010). The animals were housed two to three per cage at constant temperature and relative humidity, and were acclimated to a 12h light / 12h dark cycle and had *ad libitum* access to food and water. All animal procedures were approved by the Ethics Committee on Animal Use of University of Naples “Federico II” (permission number 363/2016-PR, prot. 39F3A.0) and comply with the standards of the European Union.

3.3 Anatomical analysis of mouse brain

Macro-morphological analysis of brain structural alterations has been performed in 14 (7 *prep1*$^{i/+}$ and 7 WT) male 6-months-old mice. Mice have been euthanized and perfused with phosphate buffered saline (PBS). The brains have been rapidly resected, fixed in 4% paraformaldehyde for 1h at room temperature. Images were obtained by Chemidoc (Bio-Rad®) and morphological differences were analysed by ImageJ® software, adding a scale bar of 3 mm.

3.4 Hemalum staining

Olfactory bulbs (OBs) extracted from 7 *prep1*$^{i/+}$ and 7 WT male six months-old mice were fixed in 4% paraformaldehyde for 1h at room temperature, cryoprotected in a 20% sucrose solution for 2h and embed in OCT (Optimal Cutting Temperature) compound prior to frozen sectioning on a microtome-cryostat. OBs 20µm coronal cryo-sections were incubated with Mayer Hemalum staining solution for 10min at room temperature, rinsed with H_2O for 5min, dehydrated in ethanol decreasing scale and soaked in xylene. Slices were mounted in Eukitt and images were obtained with digital microscope-camera (Leica®) (original magnification 10X). Images were analysed by ImageJ® software, adding a scale bar of 50µm.

3.5 Cytochrome C Oxidase (COX) staining

OBs extracted from 7 *prep1*$^{i/+}$ and 7 WT male six months-old mice were fixed in 4% paraformaldehyde for 1h at room temperature, cryoprotected in a 20% sucrose solution for 2h and embed in OCT compound prior to frozen sectioning on a microtome-cryostat. OBs 20µm coronal cryosections were

incubated at 37°C for 2h in a staining solution containing: 24.4mg of bovine Cytochrome C, 125mg of 3,3'-Diaminobenzidine (DAB), 4.5g of sucrose, 1mL Dimethyl sulfoxide (DMSO) and 50µL of bovine catalase in 0.1 M pH 7.4 HEPES buffer. Sections were, then, embed in 4% paraformaldehyde for 1h at room temperature, rinsed with PBS, dehydrated in ethanol and soaked in xylene. Slice were covered with a glass coverslip and images were obtained with digital microscope-camera (original magnification 5X). ImageJ® program was used for images analysis adding a scale bar of 100µm.

3.6 Image analysis

Images were quantitatively analysed using ImageJ® software freely available at http//imagej.en.softonic.com. For cell count measurement, images were converted to 8-bit, thresholded, segmented using a watershed filter and the number of particles automatically counted using the "Analyse particles" plug-in. Periglomerular cells number is expressed as the number of cells per area, considering as ROI the glomerular layer. Mitral and Granule cells number is expressed as number of cells per unit length, due to the distribution of these cells on a single layer and not on an area. The number of olfactory glomeruli was manually counted and expressed as number of glomeruli per unit area. For COX activity quantification, the mean optical density (defined as –log (mean grey level/256) was measured at level of the glomerular and the external plexiform layer. COX activity in the mitral cell layer has not been measured due to the imprecision in identifying this region using this histochemical method.

3.7 Behavioural tests

Behavioural monitoring was performed on male *prep1*$^{i/+}$ (n= 9) and WT littermates (n= 9) at the age of 6 months, during the light phase between 10:00 a.m. – 5:00 p.m. A modified SHIRPA protocol has been used as a first screening to observe gross abnormalities in posture and sensorial response. The presence of foot clasping (abduction of hind-limbs) has been evaluated suspending mice by their tails. Subsequently, mice have been tested for their negative geotaxis in order to underline alterations in motor abilities. A minimum of one day separated the testing sessions.

3.7.1 Negative geotaxis and climbing

Mice were placed on the lower part of an inclined grid (13cm wide, 50cm high, 60° inclination, 12mm mesh, borders covered by tape), facing the floor. The time to turn (negative geotaxis) and to reach the top of the grid was recorded, with a maximum time of 5 min.

3.7.2 Open field

Mice were placed in the middle of a clear Plexiglas (50x50x25cm^3) chamber and allowed to explore the novel environment for 5 min. The arena has been subdivided in nine square regions and the number of entries in adjacent square regions was counted off line as index of total locomotor activity. The number of entries in the central region (30x30cm^2) was also separately measured. Number of entries in adjacent square regions-to number of entries in the central region ratio was considered as an index of anxious-like behaviour.

3.7.3 Olfactory assessment

To assess olfaction, olfactory perception test was performed on 12h-fasting *prep1*$^{i/+}$ and WT mice. 1h prior to test, mice have been habituate by placing their cage in the testing room with no water bottle. Animals were placed in the clean assigned cage and let it explore for 5min until the environment of the experimental cage was familiar to the home cage (habituation). The odorant stimuli were tap water (neutral odour), cinnamon in H_2O (1% w/v) and peanut butter in peanut oil (10% w/v). These two odours scents were selected as favourite among nine different odours scents (i.e. orange, lemon, vanilla, strawberry, banana, cinnamon, lavender, peanut and mint) based on preliminary novel odour recognition trials with other C57BL/6J mice (data not shown). After habituation, immediately 20µl of selected scents (cinnamon or peanut butter) and 20µl of the neutral scent (tap water) were spotted on blotting paper (5x5cm) and placed onto the opposite walls of the cage. Mice were allowed to explore the odours for a total of 3min. An experimenter recorded the cumulative time that the mice spent sniffing the different scents. Measurement of olfactory perception was performed by comparing the times (sec) spent with the odours subtracted to the time spent with water between the genotypes.

3.8 Cell culture procedures and transfection

Mouse neuroblastoma cells (N2A) were cultured at 37°C in Dulbecco's modified Eagle's medium (DMEM) supplemented with 10% fetal bovine serum (FBS), 2% L-glutamine, 10,000 units/ml penicillin, 10,000 g/ml streptomycin. Transient transfection of Prep1 plasmid cDNA (PRC/CMV-*prep1*) was performed by using Lipofectamine 2000 reagent according to the manufacturer's instruction. For these studies, 60-80% confluent cells were washed twice with Optimem (Invitrogen) and incubated for 8h with 2-5g of plasmid construct and

6-15µL of lipofectamine reagent. The medium was then replaced with DMEM with 10% FBS and cells further incubated for 15h before being assayed.

3.9 Western blot analysis

Tissue samples were homogenized in a Polytron (Brinkman Instruments, N.Y.) in 20ml T-PER reagent/gram of tissue according to manufacture (Pierce, IL). After centrifugation at 10,000 rpm for 5 minutes, supernatant was collected. Cells were solubilized in lysis buffer (50 mmol/L HEPES, pH 7.5, 150 mmol/L NaCl, 10 mmol/L EDTA, 10 mmol/L $Na_4P_2O_7$, 2 mmol/L Na_3VO_4, 100 mmol/L NaF, 10% glycerol, 1% Triton X-100, 1 mmol/L PMSF, 10 mg/mL aprotinin) for 1h at 4°C and lysates were centrifuged at 14,000 rpm for 20 min. Total homogenates were separated by SDS-PAGE and transferred on 0.45 m Immobilon-P membranes. Upon incubation with primary and secondary antibodies, immunoreactive bands were detected by ECL according to the manufacturer's instructions.

3.10 Real-Time (RT-PCR) analysis

Total RNA was isolated from brain tissue and N2A cells by using the QIAGEN RNeasy kit (QIAGEN Sciences, Germany), according to manufacturer’s instructions. 1µg of tissue or cell RNA was reverse-transcribed using Superscript III Reverse Transcriptase (Invitrogen, CA). PCR reactions were analyzed using SYBR Green mix (Bio-Rad®, Hercules, CA). Reactions were performed using Platinum SYBR Green qPCR Super-UDG using an iCycler IQ multicolor Real-Time PCR Detection System (Bio-Rad®, Hercules, CA). All reactions were performed in triplicate and *β-actin* was used as an internal standard. Primer sequences used were as follows:

human/mouse Prep1 (*prep1*)	F:5'-GGAGTGCCAACCATGTTAAGAAGAAGTCCC-3' R: 5'- GACACCGTGTGCTTCTCGCTCAAG-3'
mouse IGF-1R (*igf1r*)	F: 5'- GCACCAATGCTTCAGTCCCT- 3' R: 5'- TTGGAGCAGTAGTTGTGCCG - 3'
mouse TrkB (*ntrk2*)	F: 5'-TCACTTCGCCAGCAGTAGC-3' R: 5'-CTCAGGGCTGGGGAGCAAC-3'
mouse $p75^{NTR}$ (*ngfr*)	F: 5'-AGGGGTGTCCTTTGGAGGT-3' R: 5'-CAGAGAACGTAACACTGTCCA-3'
mouse *β-actin*	F: 5'- CGCCCTAGGCACCAGGGTGTG - 3' R: 5'- TCGGTGAGCAGCACAGGGTG - 3'

3.11 Cell proliferation assay

N2A cells were seeded in 12-well culture plates at a concentration of 5 x 10^4 cells/mL in a complete medium and transiently transfected with Prep1 plasmid cDNA, as previously reported in 3.8. After 24, 32, 48 and 72 hours from transfection, cells were centrifuged at 1500 rpm for 5 min and then resuspended in DMEM 10% FBS. Cell count has been performed either by Bürker chamber and with the TC10TM Automated Cell Counter (Bio-Rad®, Hercules, CA) according to the manufacturer's protocol. Three replicate wells were used for each data point, and the experiment was performed three times.

3.12 Cell viability assay

N2A cells (5 x 10^4 cells/mL) were seeded into 12-well plates in complete medium and transiently transfected with Prep1 plasmid cDNA, as reported in 3.8. After 48 hours from transfection, cell viability was assessed by

Sulforhodamine B assay. Briefly, the cells were fixed with 50 % trichloroacetic acid for at least 2 hours at 4°C. Then, cells were washed 5 times with distilled and de-ionized water. After air-drying, cells were stained for 30 minutes with 600µl 0.4% Sulforhodamine B dissolved in 1% acetic acid. Unbound dye was removed by five washes with 1% acetic acid. After air-drying, 10mM Tris solution (pH 7.5) was added to dissolve the protein-bound dye. Cell density was assessed by optical density determination at 510 nm using Infinite® 200 PRO plate-reader (Tecan Trading AG, Switzerland). Three replicate wells were used for each data point. Each experiment was performed three times.

3.13 [U-^{14}C]glucose uptake assay

N2A cells (5 x 10^4 cells/mL) were seeded into 12-well plates in complete medium and transiently transfected with Prep1 plasmid cDNA, as reported in 3.8. After 48 hours from transfection, glucose uptake was measured. Cells were serum-starved for 2 hours, washed in PBS and incubated with [U-^{14}C]glucose (0.5µCi/mL) at 37°C on shaking. Following 15 min of incubation, cells were washed twice with cold PBS, subsequently lysed with 500µL 0.2 M NaOH and incubated for 30 min at 60°C. 400µL of each samples were put in tubes with dinonylphthalate oil and spinned to separate the cells with aqueous phase. Scintillation liquid was added to the collected cells for the measurement of [U-^{14}C]glucose on a beta-counter (Beckman Coulter Ireland, Inc., Indianapolis, IN). 100µL were used for determine protein concentration using Bradford Protein Assay (Bio-Rad®) method. In each experiment each treatment was determined in triplicate and normalized to the protein concentration.

3.14 Statistical procedures

Data were analysed with the Graphpad Prism 5.04 software (Graphpad Inc., San Diego, CA, USA); comparisons between *prep1*$^{i/+}$ and WT mice, and between N2A and N2A^{prep1} cells were performed via two tail Student-s t-test for unpaired data. *p* values equal or less than 0.05 were considered statistically significant.

4. RESULTS

4.1 *In silico* analysis of Prep1 expression in adult mouse CNS

In order to identify Prep1 expression in different areas of adult mouse Central Nervous System I firstly performed *in silico* analysis on Bio-GPS® and Allen Brain® web-based atlases. As shown in figure 6, *in situ* hybridization and immunofluorescence data, reported in the atlases, revealed that Prep1 transcript and protein are widely expressed in several regions of adult mouse brain but in particular within the olfactory bulb (OB) (Figure 6).

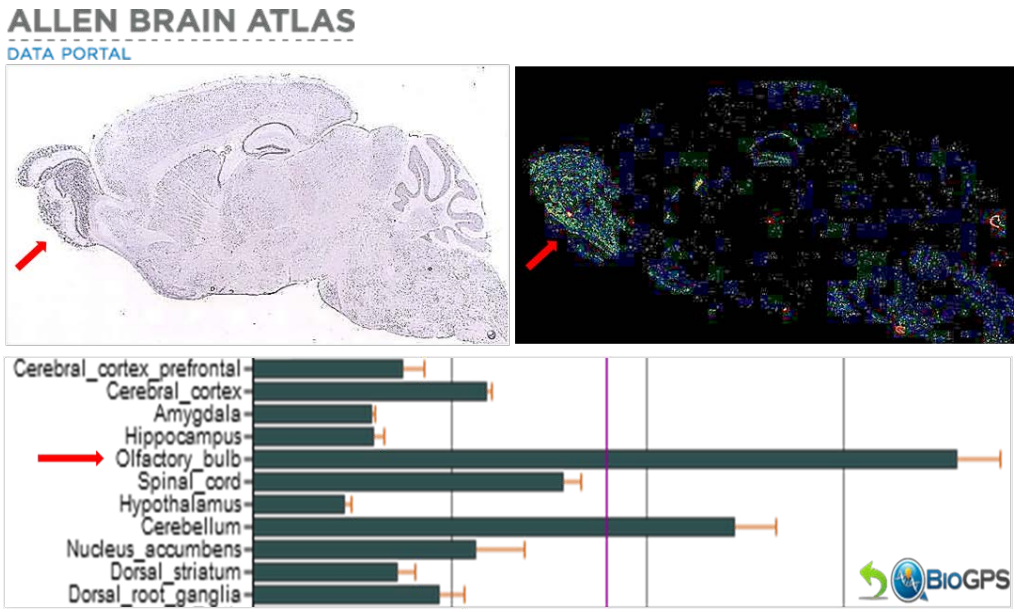

Figure 6: *In silico* Prep1 expression analysis in adult mouse brain regions
In situ hybridization and immunofluorescence evaluation of Prep1 expression on sagittal section of C57BL/6J mouse brain, reported on Allen Brain Atlas® (www.brain-map.org) and BioGPS® (www.biogps.org)

Consistent with *in silico* data, western blot analysis of male six months-old C57BL/6J mouse brain revealed that olfactory bulb represents the brain region

with the highest level of Prep1 mRNA (Figure 7A) and protein (Figure 7B), compared to other regions including cerebral cortex (CX), cerebellum (CB), hippocampus (HIPP) and hypothalamus (HYP).

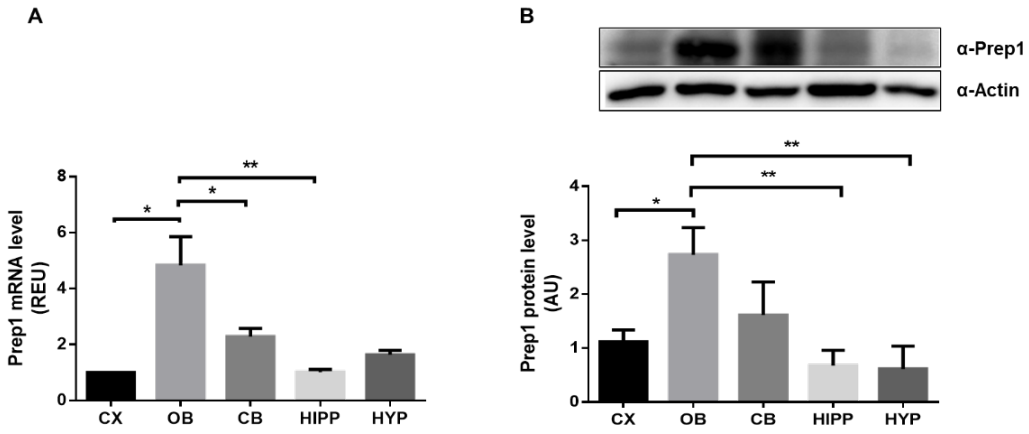

Figure 7: Prep1 mRNA and protein levels in adult C57BL/6J brain regions

A: The abundance of Prep1 mRNA was determined by RT-PCR analysis of total RNA isolated from the different brain regions of 6-month-old C57BL/6J mice, using *β-actin* as internal standard. Bar represents the mean ± SEM of three independent experiments, in each of which reactions were performed in triplicate using the pooled total RNAs obtained from five mice. B: Brains from 6-month-old C57BL/6J mice were dissected, solubilized, and protein samples were analysed by Western blot with α-Prep1 antibody. Actin antibody was used for normalization. Blot were revealed by ECL and autoradiograph subjected to densitometric analysis. The autoradiographs are representative of four independent experiments. Asterisks denote statistically significant differences (*$p<0.05$,**$p<0.01$).

4.2 Macro-morphological analysis of Prep1 deficient mouse brain

To understand the role of Prep1 in olfactory bulb, I initially performed a macro-morphological evaluation of the eventual differences in total brain structure in male 6-months-old Prep1 hypomorphic (*prep1*$^{i/+}$) and WT mice (7 mice for genotype). As shown in figure 8, anatomical analysis indicated that

prep1$^{i/+}$ mice display a significant 30% reduction of OBs area compared to WT mice. On the contrary, no significant differences were detected between the other structures, such as cerebral cortex and cerebellum (Figure 8).

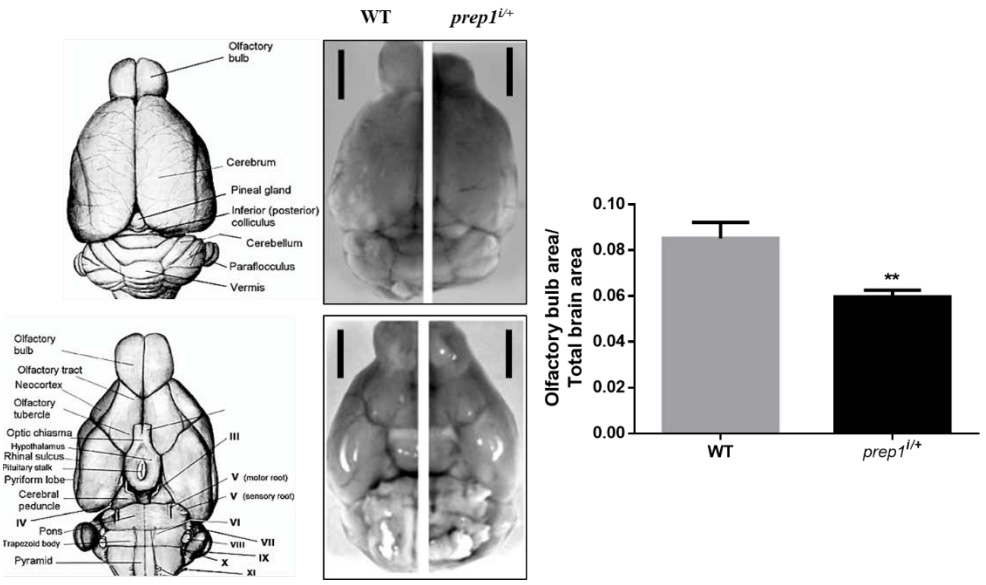

Figure 8: Anatomical analysis of *prep1*$^{i/+}$ mouse brain

WT and *prep1*$^{i/+}$ mice were euthanized, perfused and tissues were rapidly extracted and fixed in 4% paraformaldehyde. Images were obtained by Chemidoc (Bio-Rad®) and morphological differences were analysed by ImageJ® software using a scale bar of 3mm. Results are expressed as ratio of olfactory bulb area on total brain area. Bar represents the mean ± SEM of 7 mice per genotype. Asterisks denote statistically significant differences (**p<0.01).

4.3 Histological analysis of Prep1 deficient mouse olfactory bulb

In order to better characterize the anatomical abnormality observed in *prep1*$^{i/+}$ mouse brain, olfactory bulb cryosections obtained from seven 6-months-old *prep1*$^{i/+}$ mice and seven WT littermates were analysed by Hemalum (hematoxylin&eosin) staining. Histological analysis showed that Prep1 deficient mice display a normal morphological structure of olfactory bulb with no significant difference in the width of the layers. However, histochemical staining

revealed significant differences in olfactory cells number between two genotypes. Count density measurement showed that *prep1*$^{i/+}$ mouse OB displays a significant 30% reduction of periglomerular cells number than WT mouse, accompanied by a slight reduction of number of olfactory glomeruli. On the other hand, *prep1*$^{i/+}$ mice feature a significant higher number of mitral cells than control animals. No significant differences in granule cells number in *prep1*$^{i/+}$ mice olfactory bulbs were observed (Figure 9).

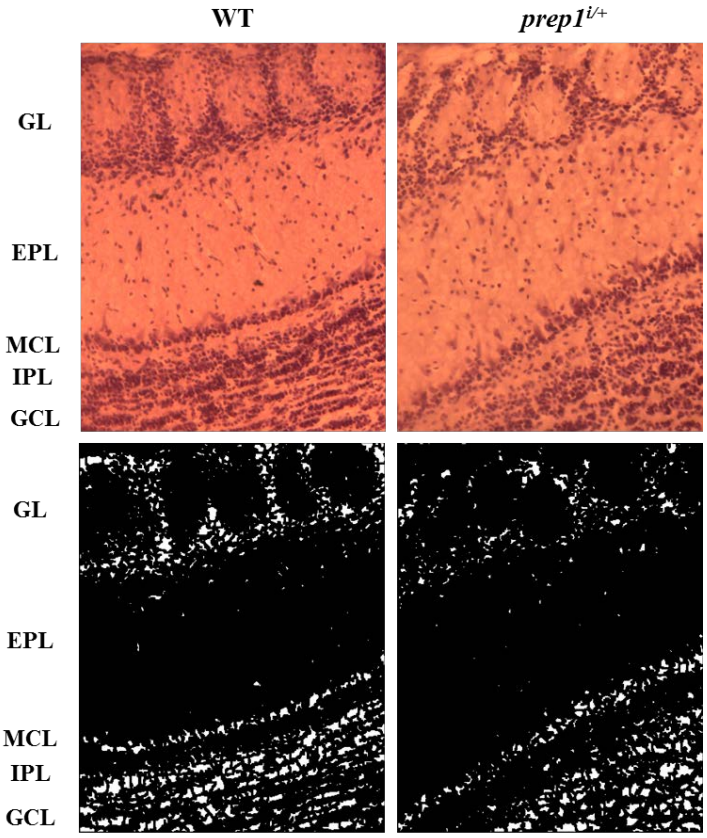

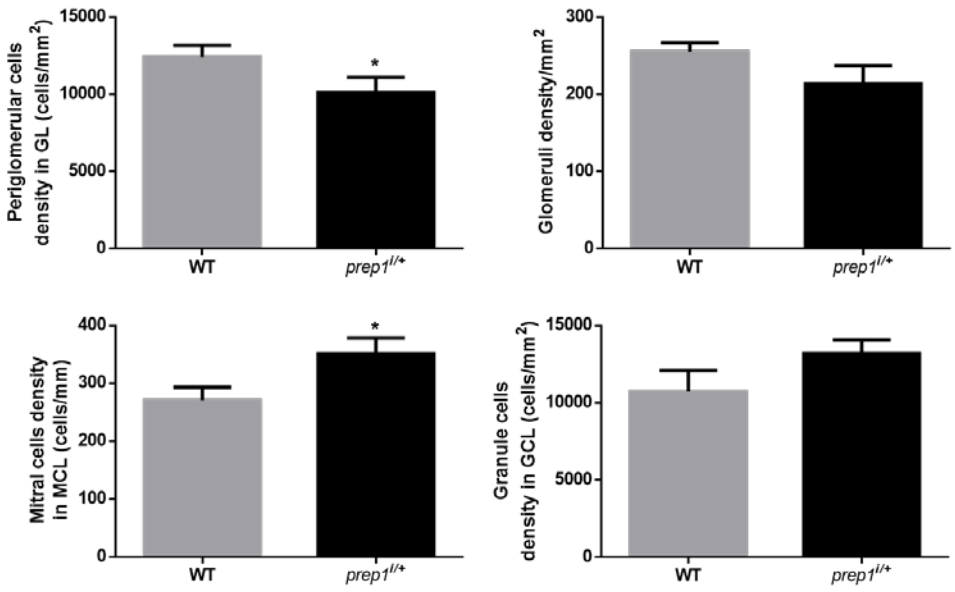

Figure 9: Hemalum staining of *prep1*$^{i/+}$ mice OBs sections

Olfactory bulb coronal cryosections from 6-months-old *prep1*$^{i/+}$ and WT littermates were stained with Hemalum. ImageJ© program was used for cell number evaluation (original magnification 10X) using a scale bar of 50µm. The graphs shown are representative of findings observation in 7 *prep1*$^{i/+}$ and 7 control animals. Asterisks denote statistically significant differences (*$p<0.05$). Abbreviations: GL, glomerular layer; EPL, external plexiform layer; MCL, mitral cell layer; IPL, internal plexiform layer; GCL, granule cell layer.

To verify whether the reduced quantity of periglomerular cells, as well as the increased number of mitral cells, observed in Prep1 deficient mice, might affect neuronal function in terms of metabolic activity, OB cryosections from *prep1*$^{i/+}$ and WT mice (7 mice per genotype) were analysed by Cytochrome C oxidase (COX) staining, which is able to indirectly quantify cell metabolism by measuring the enzymatic activity of the main enzyme involved in mitochondrial OXPHOS (COX).

In the olfactory bulb, COX activity has been described to be mainly present within the glomerular layer, where periglomerular cells axons and olfactory fibers converge, and in the external plexiform layer (EPL) where mitral

and tufed cells axons converge (Mouradian LE and Scott JW, 1988). Therefore, we quantified COX activity in glomeruli and in the external plexiform layers.

As shown in figure 10, *prep1*$^{i/+}$ mice display a significant 20% reduction of COX activity within the glomerular layer compared to WT mice. A feeble and not statistically significant reduction of COX activity was observed also within the external plexiform layer (Figure 10).

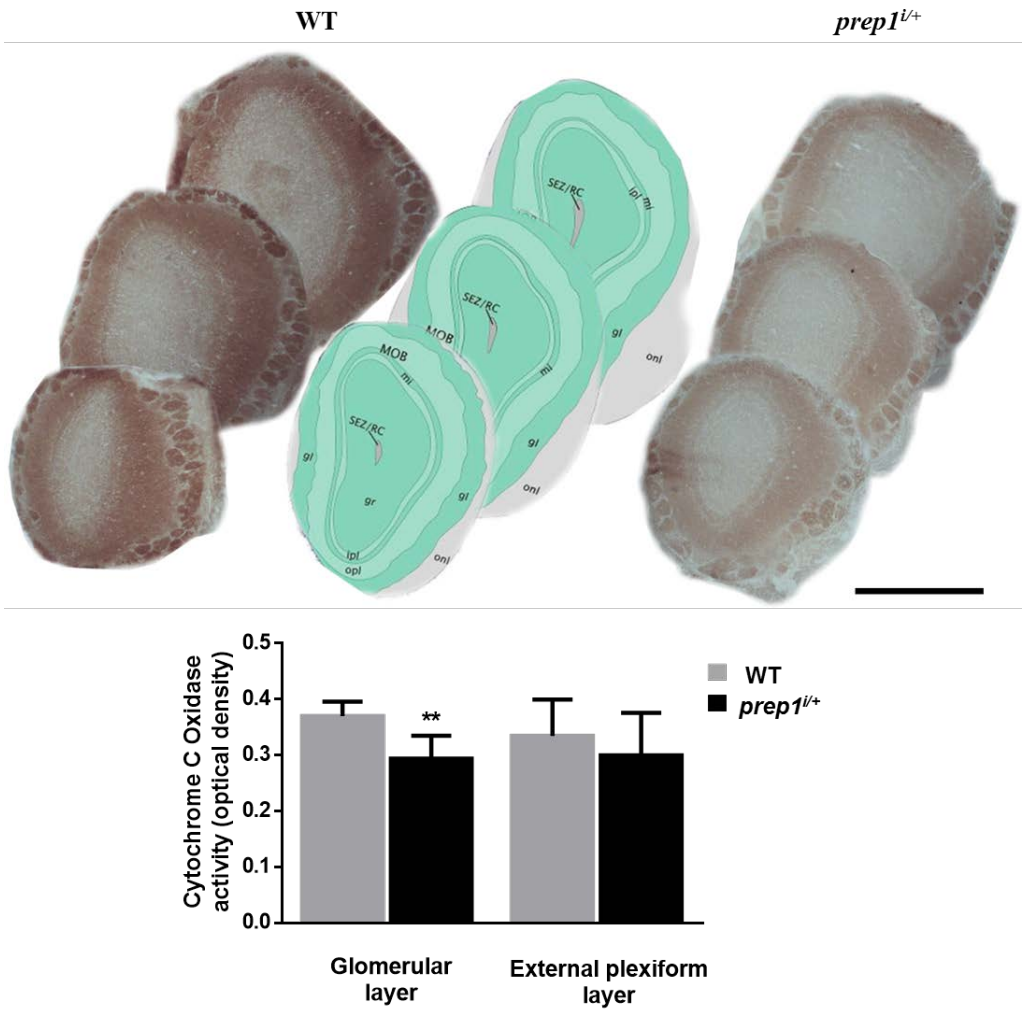

Figure 10: COX staining of *prep1*$^{i/+}$ mice OBs sections

COX staining on olfactory bulb coronal cryosections from 6-months-old *prep1*$^{i/+}$ and WT littermates was performed (n=7 per group). Measurement of COX activity was performed by ImageJ® software (original magnification 5X; scale bar 100µm). Representative images of COX

staining of olfactory bulb from *prep1*$^{i/+}$ and WT mice are shown. Reference drawings have been adapted from Allen Brain Reference Atlas®. Abbreviations: gl: glomerular layer; gr: granular layer; opl: outer plexiform layer; ml: mitral layer; ipl: inner plexiform layer; onl: olfactory nerve layer; MOB: main olfactory bulb; SEZ/RC: sub-ependymal zone. Bars represent mean±SEM of COX optical density in different olfactory bulb layers. Asterisks denote statistically significant differences (**p<0.01)

4.4 Behavioural monitoring of Prep1 hypomorphic mice

In order to verify whether the reduced number and metabolism of olfactory periglomerular neurons might give rise to impaired olfactory phenotypes, I performed a behavioural monitoring of *prep1*$^{i/+}$ and WT littermates (9 mice per genotype).

To evaluate the susceptibility to depression-like state, a tail suspension test was performed. Prep1 deficient mice displayed a tail elevation comparable to WT littermates and showed a regular posture with extended hind limbs. Immobility time during suspension was similar among groups. Moreover, no differences in time to climb and negative geotaxis has come up (data not shown).

To examine locomotor activity and behavioural anxiety an open field test was administrated. A significant difference in active exploratory behaviour was noted between the two genotypes. Indeed, as shown in the figure 11, number of entries in the adjacent square regions was significantly lower in Prep1 hypomorphic mice compared to WT littermates. Prep1 deficient mice also featured a slight reduction in center square region entries, although no statistical significance was found. No variance in center to-total locomotor activity ratio has been observed, indicating absence of differences in anxious-like behaviours between the groups. (Figure 11).

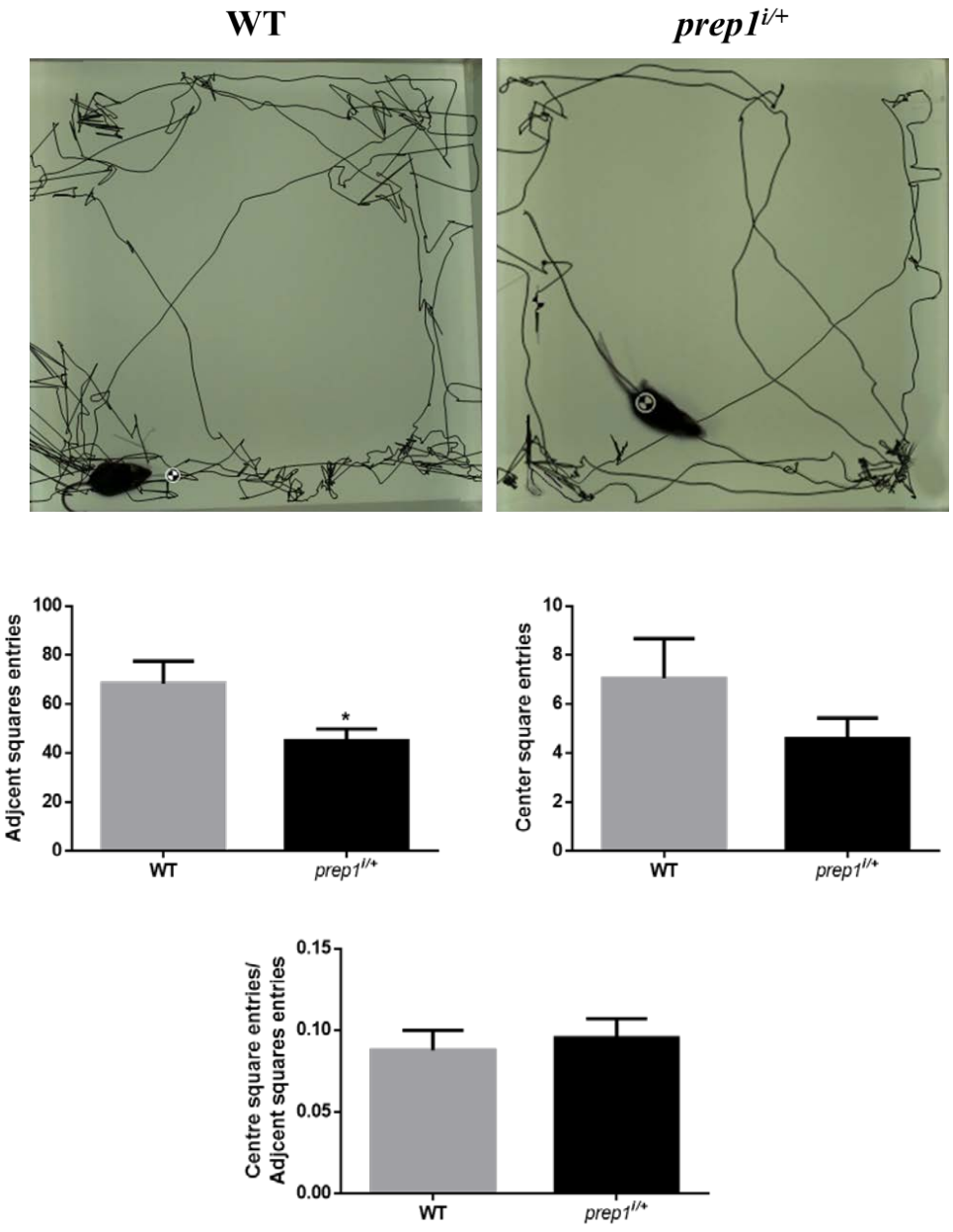

Figure 11: Open field test on *prep1*$^{i/+}$ mice

Prep1 deficient and WT mice (n = 9 per genotype) were placed in the center of a clear Plexiglas arena (50x50x25cm^3) and let them explore the environment for 5 min. Representative traces of the exploratory behaviour of WT and *prep1*$^{i/+}$ mice are shown. Locomotor activity was quantified subdividing the arena in 9 regions and counting the entries between adjacent squares; centre square entries and centre to adjacent squares entries ratio were also measured for evaluation of anxiety behaviour. Asterisks denote statistically significant differences (*$p<0.05$).

In parallel, I analysed mice olfactory detection abilities by performing olfactory perception test which measures the preference index to odorous scents (e.g. peanut butter and cinnamon). The hypomorphic and WT mice were tested and the exploratory time to discover the odours items was quantified subtracting time spent on odour to time spent on water (preference index). As shown in figure 12, the WT group displayed a higher preference to peanut butter and cinnamon than to water. On the contrary, Prep1 deficient mice showed a significantly very low attraction to cinnamon and to peanut butter, spending more time with water (Figure 12).

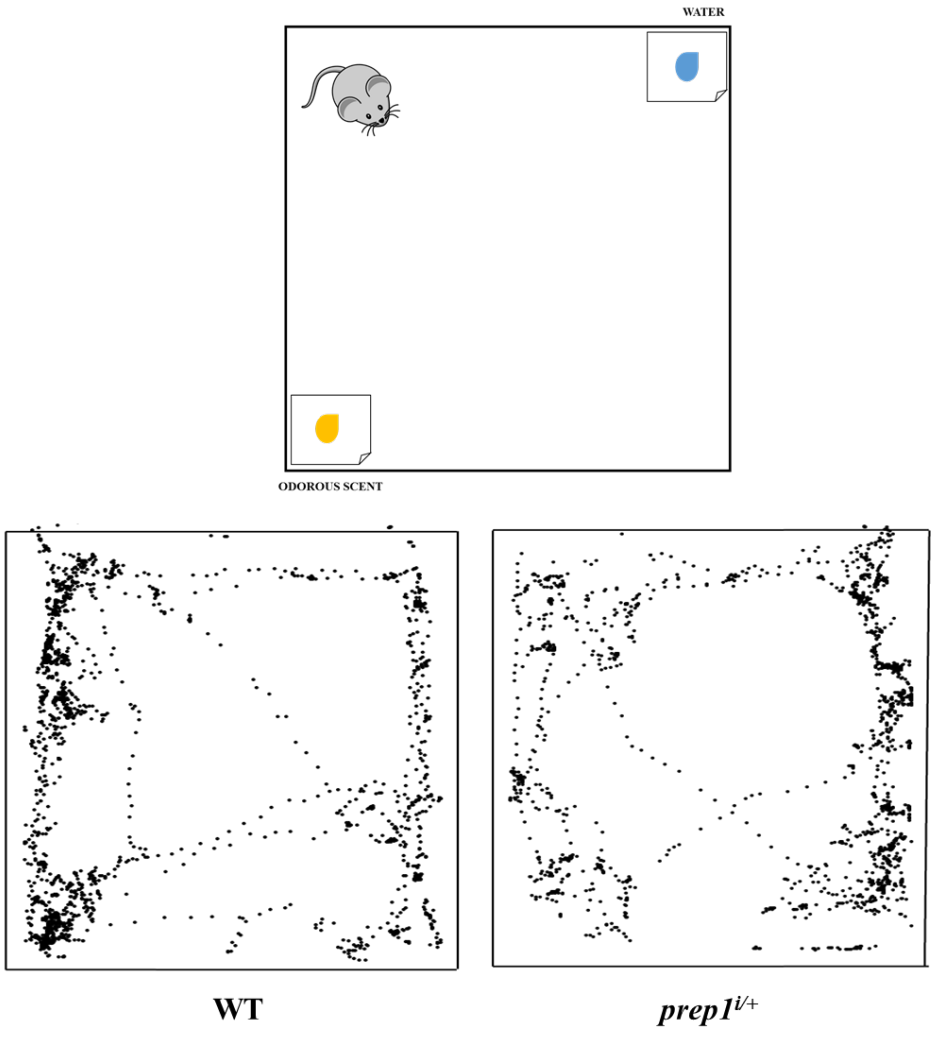

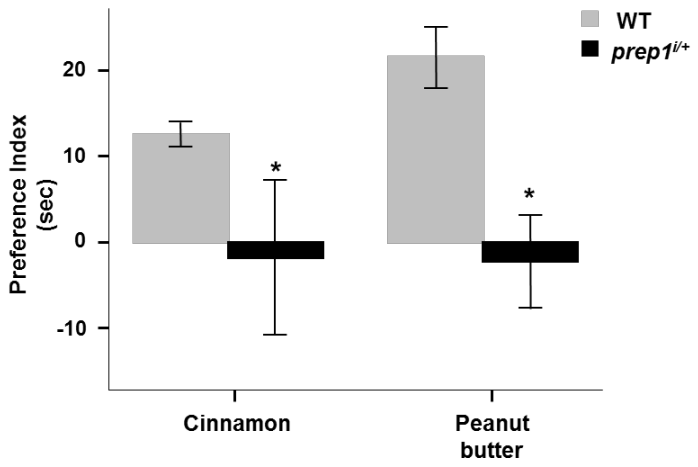

Figure 12: Olfactory assessment of *prep1*$^{i/+}$ mice

Prep1 deficient and WT mice (n = 9 per group) have been exposed for 3 min to peanut butter or cinnamon scents blotted on filter paper which has been placed on the opposite corner of a filter paper blotted with water. Representative drawing of olfactory test and the representative traces of animals exploring the arena are shown. The total time (sec) exploring the odour has been subtracted to time spent on water (preference index). Asterisks denote statistically significant differences (*p<0.05)

4.5 Evaluation of olfactory-specific neurotrophins signalling pathways

Olfactory periglomerular cells represent the main inhibitory interneurons which establish a reciprocal balance with the excitatory neurons (mitral and tufted cells) that allows the correct processing of sensorial information from olfactory epithelium through the olfactory cortex to other brain areas (Mori K *et al.*, 1999). Several evidences suggest a key role of some neurotrophic factors, such as BDNF and IGF-1 in regulating periglomerular cells differentiation from neuroblasts within the subventricular zone (SVZ) (neurogenesis) and in affecting olfactory tuning and plasticity (Arsenijevic Y and Weiss S, 1998; Bath KG and Lee FS, 2010; Nieto-Estévez *et al.*, 2016). In particular, many findings have indicated that, compared to embryonic development stages, in post-natal and adult life, commitment of SVZ-derived stem cells to the OB does not depend

upon neurotrophic factors amount but upon receptor ssensitivity of neuroblasts to the extrinsic growth factors (Bath KG and Lee FS, 2010).

Thus, in order to verify the hypothesis that Prep1 might affect olfactory bulb neurons responsiveness to BDNF and/or IGF-1 neurotrophic signals, I measured the expression levels of target receptors for BDNF (TrkB and $p75^{NTR}$) and IGF-1 (IGF-1R) in *prep1*$^{i/+}$ and WT mice OBs (7 mice per genotype). As shown in figure 13, OBs from *prep1*$^{i/+}$ mice display a significant reduction of TrkB and $p75^{NTR}$ gene and protein levels compared to WT mice, while no significant differences were found in IGF-1R amount between the two genotypes (Figure 13A and 13B).

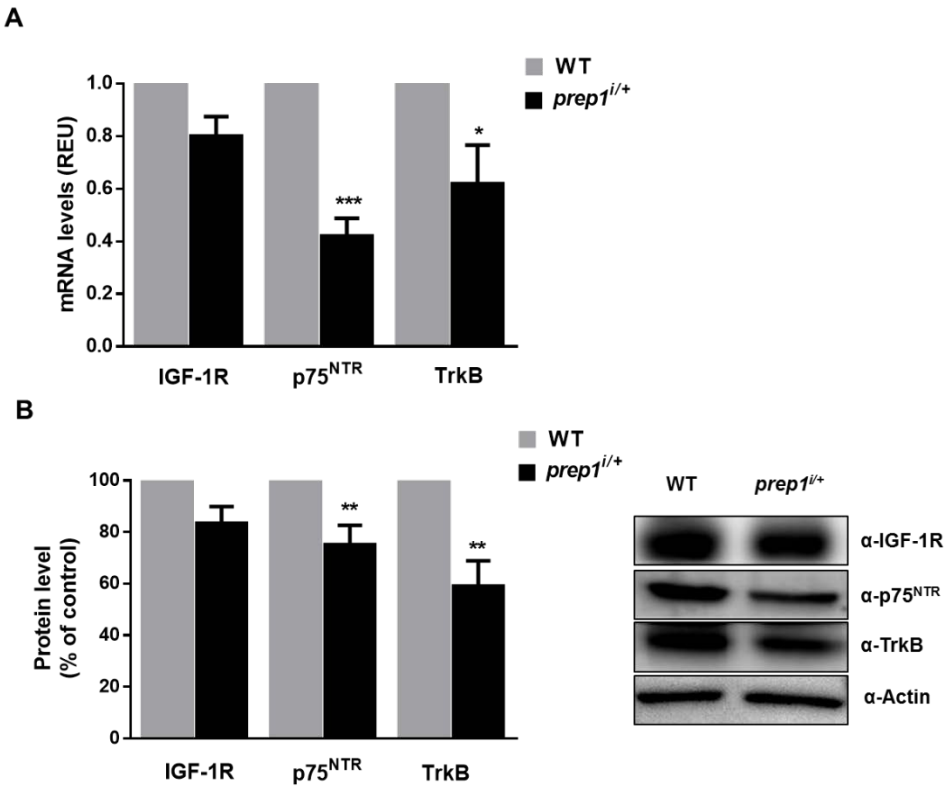

Figure 13: IGF-1R, $p75^{NTR}$ and TrkB mRNA and protein levels in *prep1*$^{i/+}$ mice

A: The abundance of IGF-1R (*igf-1r*), $p75^{NTR}$ (*ngfr*) and TrkB (*ntrk2*) mRNA was determined by real-time PCR analysis of total RNA isolated from the OB of hypomorphic and control mice, using β-actin as internal standard. Bar represents the mean ± SEM of three independent

experiments, in each of which reactions were performed in triplicate using the pooled total RNAs obtained from seven mice per genotype. B: OBs from Prep1 hypomorphic and control mice were dissected, solubilized, and protein samples analysed by Western blot with IGF-1R, $p75^{NTR}$ and TrkB antibodies. Actin antibody was used for normalization. Blot were revealed by ECL and autoradiograph subjected to densitometric analysis. The autoradiographs shown on the top of the graphic are representative of three independent experiments. Asterisks denote statistically differences (*p<0.05, **p<0.01, ***p<0.001).

Through careful *in vitro* studies, it has been demonstrated that TrkB and $p75^{NTR}$ receptors exert BDNF-mediated signalling for appropriate migration, differentiation and proliferation of neuroblasts within the olfactory area, via MAP-kinases and/or PI3-kinase, and NFκB pathways, respectively (Chiaramello S *et al.*, 2007; Reichardt LF, 2006).

To verify the hypothesis that decreased TrkB and $p75^{NTR}$ expression in Prep1 deficient mice OBs may lead to a reduction of BDNF-mediated neurotrophic signalling, I measured phosphorylation levels of the main kinases involved in TrkB signalling pathways. Western blot analysis revealed that *prep1*$^{i/+}$ mice olfactory bulbs feature a deep reduction of p-Akt/PKB^{Ser473}, p-ERK1/2$^{Thr202/Tyr204}$ and p-IκBα$^{Ser32/36}$, compared to control animals, with no difference in Akt/PKB, ERK1/2 and IκBα total protein amount (Figure 14).

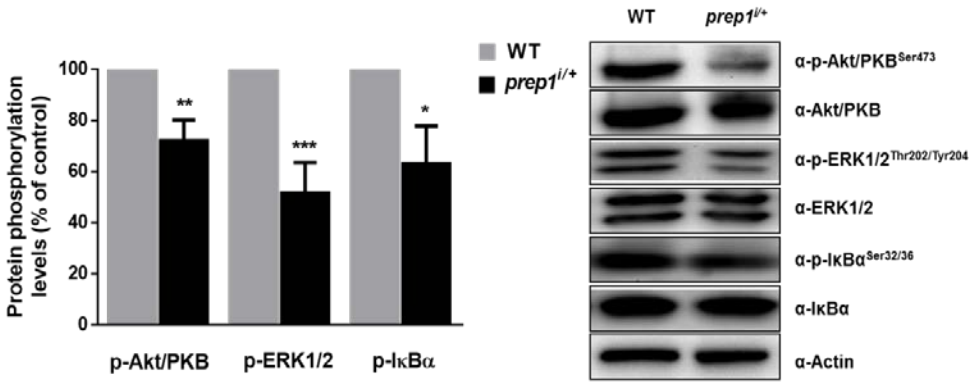

Figure 14: Akt/PKB, ERK1/2 and IκBα phosphorylation levels in *prep1*$^{i/+}$ mice

OBs from Prep1 hypomorphic (n=7 per group) and control mice were dissected, solubilized, and protein samples analysed by Western blot with p-Akt/PKB^{Ser473}, Akt, p-ERK1/2$^{Thr202/Tyr204}$,

ERK1/2, p-IκBα$^{Ser32/36}$ and IκBα antibodies. Actin antibody was used for normalization. Blot were revealed by ECL and autoradiograph subjected to densitometric analysis. The autoradiographs shown on the top of the graphic are representative of four independent experiments. Asterisks denote statistically differences (*p<0.05, **p<0.01, ***p<0.001).

4.6 Neuronal cells overexpressing Prep1: growth, viability and metabolism assessment

To further investigate the effects of Prep1 on neuronal cell proliferation and functionality, I transiently transfected Prep1 cDNA (PRC/CMV-*prep1)* or empty vector (PRC/CMV) in a mouse neuronal cell line (N2A) and differences between cell growth and viability were evaluated by growth curves at 24, 32, 48 e 72 hours and Sulphorodamine B assay, respectively. As shown in the figure, N2A cells overexpressing Prep1 (N2A^{prep1}) showed an increased cell growth which is significantly greater at 48h after Prep1 cDNA transfection, compared to control N2A cells (Figure 15A). Consistently, Sulphorodamine B assay, performed after 48h from Prep1cDNA transfection, revealed that N2A^{prep1} feature a 35% increased cell viability compared to control cells (Figure 15B).

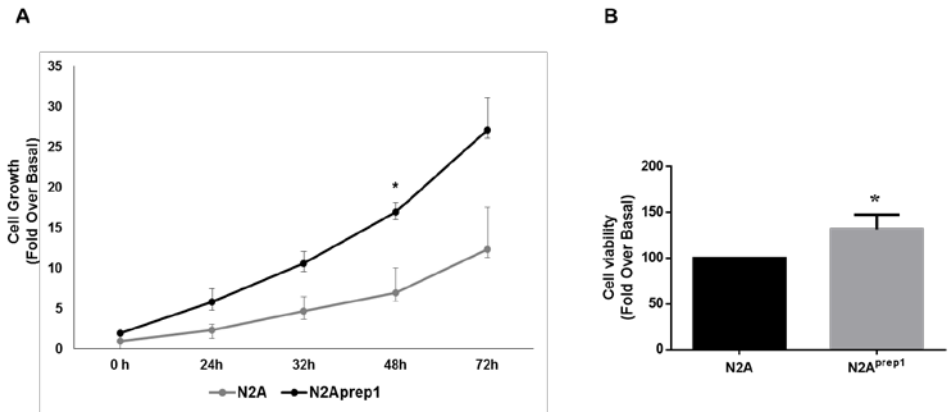

Figure 15: Cell growth and viability in N2A cells overexpressing Prep1

A: N2A cells were transiently transfected with Prep1 cDNA, as described in Material and Methods. Then, cells have been counted, either by Bürker chamber and with the TC10TM Automated Cell Counter (Bio-Rad®, Hercules, CA), and the results reported as fold-increase over basal. B: N2A cells were transiently transfected with Prep1 cDNA, as described in Material and Methods. After 48 hours from transfection, cell viability was measured by Sulforhodamine Bassay and assessed by optical density determination at 510 nm. Bar represents the mean ± SEM of four independent experiments. Asterisks denote statistically significant values (*p<0.05)

To examine whether Prep1 might directly influence neuronal metabolism, I performed [U-^{14}C]glucose uptake assay. As shown in the figure, neuronal cells overexpressing Prep1 displayed more than 2-fold increase of glucose transport, compared to control cells (Figure 16).

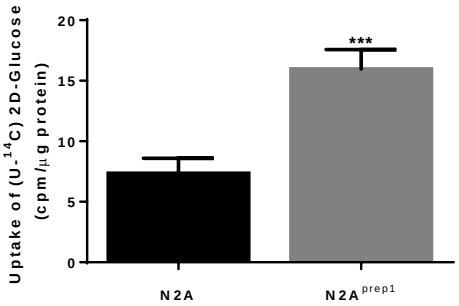

Figure 16: [U-^{14}C] glucose uptake in N2A cells overexpressing Prep1

N2A cells were transiently transfected with Prep1 cDNA, as described in Material and Methods. Then, cells were counted and aliquots were incubated with [U-^{14}C]glucose (0.5μCi/ml) at 37°C on shaking. After 15 min aliquots of each samples were put in scintillation liquid for measurement of [U-^{14}C]glucose on beta counter. Bar represents the mean ± SEM of three independent experiments, in each of which reactions were performed in quintuple. Asterisks denote statistically significant differences (***p<0.001).

4.7 TrkB-mediated signalling pathway evaluation in N2A*prep1*

In order to confirm the role of Prep1 in regulating TrkB- and/or p75-dependent neurotrophic signals I analysed TrkB and $p75^{NTR}$ gene and protein levels in N2A overexpressing Prep1 cells. Gene expression analysis showed a fleeble and no significant increase of $p75^{NTR}$ transcript (Figure 17A) in N2A*prep1* cells compared to control ones, while a significant 4-fold increase of TrkB gene was observed (Figure 17B). Consistently, Western blot analysis revealed a low increase of $p75^{NTR}$ protein level, while a significant 2-fold increase of TrkB protein amount was noted (Figure 17C).

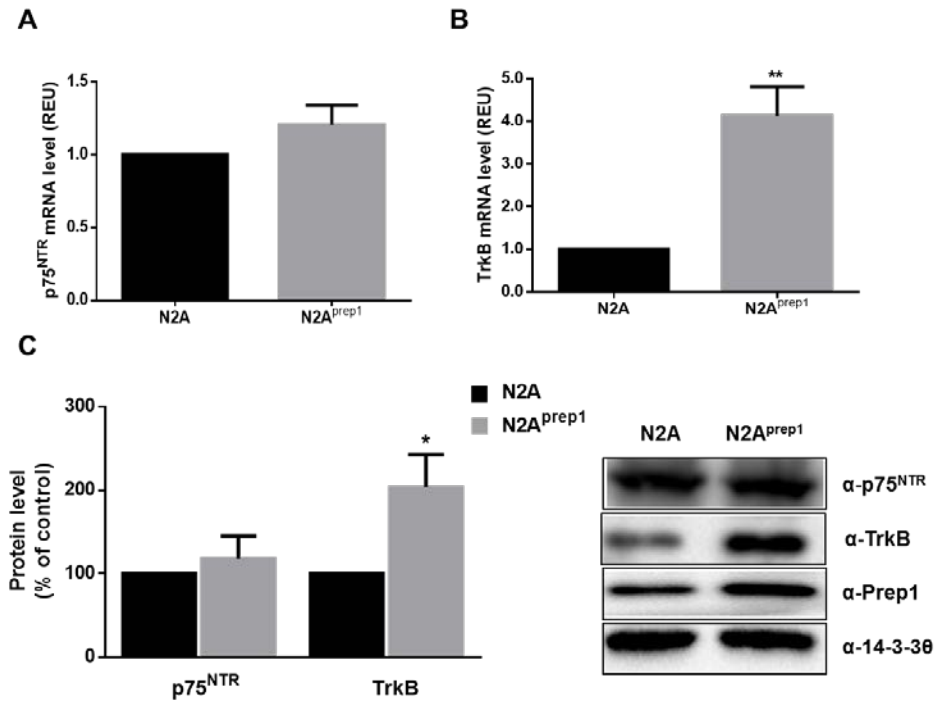

Figure 17: $p75^{NTR}$ and TrkB mRNA and protein levels in N2A cells overexpressing Prep1
N2A cells were transiently transfected with Prep1 cDNA, as described in Material and Methods. A and B: The abundance of $p75^{NTR}$ (*ngfr*) and TrkB (*ntrk2*) mRNA in N2A*prep1* and control cells was determined by real-time PCR analysis using β-actin as internal standard. Bar represents the mean ± SEM of three independent experiments. C: N2A*prep1* and control cells were lysed and protein samples analysed by Western blot with TrkB and $p75^{NTR}$ antibodies. 14-3-3θ antibody

was used for normalization. Blot were revealed by ECL and autoradiograph subjected to densitometric analysis. The autoradiographs shown on the top of the graphic are representative of three independent experiments. Asterisks denote statistically differences (*p<0.05, **p<0.01).

In addition, Akt and, in particular, ERK phosphorylation levels were found higher in N2A overexpressing Prep1 then control cells, while p-IκBα levels do not significantly change between N2A^{prep1} and control cells (Figure 18).

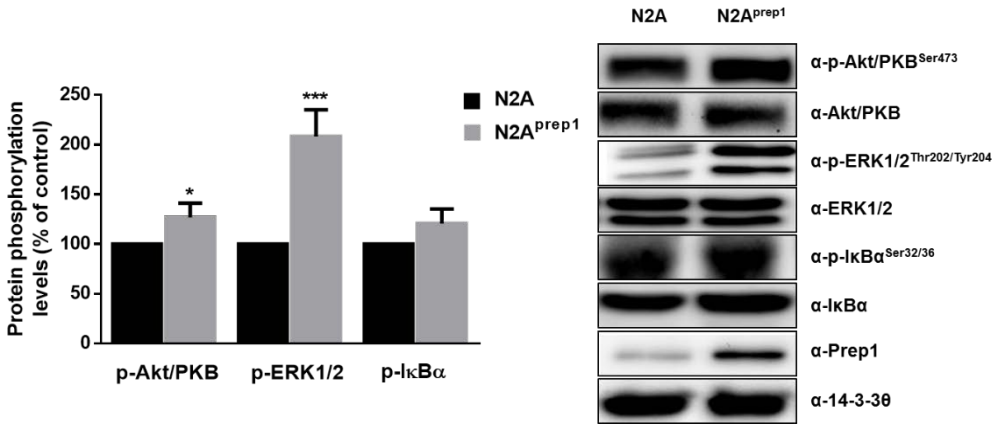

Figure 18: Akt/PKB, ERK1/2 and IκBα phosphorylation levels in N2A cells overexpressing Prep1. N2A cells were transiently transfected with Prep1 cDNA, as described in Material and Methods. N2A^{prep1} and control cells were lysed and protein samples analysed by Western blot with p-Akt/PKB^{Ser473}, Akt, p-ERK1/2$^{Thr202/Tyr204}$, ERK1/2, p-IκBα$^{Ser32/36}$ and IκBα antibodies. 14-3-3θ antibody was used for normalization. Blot were revealed by ECL and autoradiograph subjected to densitometric analysis. The autoradiographs shown on the top of the graphic are representative of four independent experiments. Asterisks denote statistically differences (*p<0.05, ***p<0.001)

5. DISCUSSION

Chemical senses result from the cells evolutionary ability to recognize exogenous molecules and to develop appropriate responses. For the majority of species, including human, the chemical senses, and in particular smell, represent a vital function, and among all the existing animal species, there is no doubt that mouse is that one which have most developed this way. Smell represents a critical sensory modality in mice, thus mouse brain presents extremely large olfactory bulbs and bulging olfactory tubercles (Hegan CE *et al.*, 2012). The olfactory bulb is the first relay structure in olfactory processing, which receives direct input from olfactory sensory neurons (OSNs) in the olfactory epithelium and sends output to the olfactory cortex and other brain areas which originate neuroendocrine responses and innate behaviour. The olfactory bulb circuitry encompasses two types of principal excitatory neurons, mitral and tufted cells, and two main inhibitory interneuron types, periglomerular (PGC) and granule cells. The cell bodies and dendrites of these neurons are organized into layers. The most superficial layer is composed of spherical structures called glomeruli, in which the axons of OSNs make glutamatergic synapses with primary dendrites of mitral/tufted (M/T) cells and PGC cells (Arruda D *et al.*, 2013). A unique characteristic of the olfactory sensory system, described in all vertebrates, is the continuous replacement of the olfactory neurons during the lifetime. Within the OBs there is a substantial amount of new-born neurons which originate from progenitor cells in the subventricular zone (SVZ) and migrate along the rostral migratory stream (RMS) to become functional interneurons in the OB (Hagg T, 2005). The combination of genes that regulates proliferation and cell fate determination of SVZ precursors remains to be identified, although neurogenesis steps have been described to be regulated in large part by neurotrophic factors, such as IGF-1 (Vogel T, 2013) and BDNF. In particular, BDNF by acting on $p75^{NTR}$ and TrkB downstream receptors, promote

migration, survival and differentiation of new-born cells integrated in the OB (Yuan TF, 2008). Previous studies demonstrated that newly generated neurons in olfactory bulb participate in fine odour discrimination, and that BDNF-haploinsufficient or TrkB-haploinsufficient mice did not spontaneously discriminate between odorants, suggesting that BDNF activity significantly impact olfactory abilities (Bath KG *et al.,* 2012). However, these data remain correlative and the detailed mechanisms underlying these BDNF-related olfactory deficits are still unknown. Prep1/Pknox1 is a member of transcription factors TALE superfamily which play an irreplaceable function in the early and late stages of development and remain active also during the post-natal life. In rodents CNS development, Prep1 has been observed to represent a key co-factor of homeodomain proteins Pbx1, Hoxb1 and Meis involved in hindbrain formation. Stable expression and activity of these Prep1 co-factors, however, have been detected also in many regions of adult brain, especially in olfactory sensory areas (Parrilla M *et al.,* 2016). By *in situ* hybridization on rat brain, Redmond L localized high expression levels of Pbx1 postnatally in the SVZ, in the migratory pathway to the olfactory bulb and in the OB layers that are the targets of these migratory neurons, suggesting a role for Pbx1 in the generation of olfactory bulb interneurons (Redmond L *et al.*, 1996). Similarly, Agoston Z demonstrated that in C57BL/6J mice, Meis2 is strongly expressed in neuroblasts of the SVZ and RMS, as well as in some of the OB interneurons. Meis2, by forming ternary complex with Pax6 and Dlx2, indeed, cooperates in generation of dopaminergic periglomerular neurons in the OB (Agoston Z *et al.,* 2014). Unlike to other homeobox factors, very scant speculation has been done on Prep1 function in senso-olfactory brain regions and whether Prep1 misexpression may affect neurogenesis-dependent olfactory activity. In my study, I managed to clarify the involvement of Prep1 in adult mouse brain functions. To reach this aim I used a Prep1 hypomorphic C57BL/6J mouse model, which express ubiquitously 55-57% of the protein. According to information reported in literature and web-atlases (e.g. Allen Brain Atlas®, BioGPS®) Prep1 mRNA

and protein expression in 6-months C57BL/6J mice is particularly high in olfactory nuclei compared to other brain regions. Such marked expression might suggest a key biological function of this transcription factor in olfactory sensory circuit or olfactory renewal processes, which are inevitably related. Consistently with this hypothesis, anatomical comparison of WT and Prep1 deficient mice brains highlighted an impaired formation of olfactory bulb in *prep1*$^{i/+}$ mice, since OBs area is significantly reduced compared to control animals. By histological examination, a significant difference in the cytoarchitecture of the olfactory bulb between hypomorphic and WT mice was observed. *prep1*$^{i/+}$ mice showed a reduction in the overall number of adult-generated periglomerular cells (PGCs) which is accompanied to an increase in the mitral cells number. However, neuronal metabolic analysis of olfactory bulb layers in which PGCs and mitral cells converge, revealed a significant reduced Cytochrome C oxidase activity in the glomeruli layer of hypomorphic mice then control littermates. Within the olfactory bulb, the glomerular activity pattern is represented by the intricate interplay between output and input neurons, which define a balanced circuit that allows odorant identity and recognition. Indeed, OSNs axons release glutamate to post-synaptic glutamatergic M/T neurons, which activate PGCs. In turn, PGCs send GABAergic inhibition back to all of them, as well as to neighbour periglomerular cells (Imai T, 2014). This interneurons population plays important roles in regulating neural excitability in the bulb, thus, it is plausible to hypothesize that the imbalance in olfactory bulb cells and, in particular, the substantial reduction of PGCs number and oxidative metabolism in Prep1 deficient mice might give rise to impaired sensitivity or odour-discrimination capability. To verify this hypothesis, I performed olfactory assessment in hypomorphic and control mice. The present behavioural study showed that Prep1 deficient mice deviate substantially from WT mice in their persistence in investigating attractive odours and in their ability of spontaneously discriminate between odours. Indeed, hypomorphic mice displayed reduced response to cinnamon and peanut butter olfactory stimuli during olfactory

perception test, which may be the result of disturbed olfaction probably due to changes in synaptic connectivity that diminish odour discrimination ability. Unexpectedly, behavioural monitoring during open field exploration also revealed that *prep1*$^{i/+}$ mice feature a significant low locomotor activity. Alterations in odour preference behaviour associated to partial hypokinesia have been previously widely speculate in the study of neurodegenerative phenotypes of Parkinson Disease (Taylor TN *et al.*, 2010) and Huntington Disease (Guimaraes IM *et al.*, 2015), suggesting that impairment of olfactory-based information processing might arise from degenerative mechanisms that mostly affect higher cortical regions and limbic area. Previous studies, indeed, described that the olfactory bulb is implicated in certain types of olfactory learning and memory, and that the natural replacement of bulbar interneurons may be programmed to occur after the transferal of the memories held by these neurons to other parts of the brain (Gheusi G *et al.*, 2000). In addition, hyposmia is also a main characteristic of Kallamann Syndrome, a neuroendocrine human disease caused by lack of gonadotropin-releasing hormone (GnRH) (Whitlock KE, 2015), which has been observed to be regulated by a multimeric complex comprising the POU transcription factor Oct1 together with Prep1 and Pbx1b (Rave-Harel N *et al.*, 2004). Affection of olfactory ability and anatomic-cytological alterations in OB of Prep1 deficient mice lead me to investigate the possibility that these phenotypes may be linked to neurotrophins malsignalling on olfactory plasticity. As previously described, BDNF-mediated TrkB and p75^{NTR} signalling was observed to be essential for renewal and integration of adult-born PGCs in the OB, which are directly related to olfactory function. In agreement with previous findings, measurement of OB TrkB and p75^{NTR} levels revealed that hypomorphic mice display a significant reduced gene and protein expression of both receptors, compared to control littermates, accompanied to a lower activation of the main second messengers: Akt and ERK kinases, and NFκB.

To further verify that the observed phenotypes are attributable to the different action/expression of Prep1, I used a mouse neuronal cell line (N2A) transfected with Prep1 cDNA, which mirrors the opposite situation occurring in mouse model. Consistently, N2A overexpressing Prep1 displayed an increased proliferation and viability, with an increased glucose uptake, defining a potentially increased neuronal metabolism and activity. Molecular analysis of neurotrophic receptors TrkB and $p75^{NTR}$ revealed that $N2A^{prep1}$ present a significant increase of TrkB mRNA and protein expression compared to control cells, with a concomitant increased phosphorylation of Akt/ERK kinases. The variance from *in vivo* observations might probably be due to the lack of specific neurotrophic stimulation in N2A cells culture media. Indeed, previous studies by Gascon E observed that only application of exogenous neurotrophins, and in particular of BDNF, in SVZ neuroblasts culture media is able to favour $p75^{NTR}$ expression and activation (Gascon E *et al.*, 2005).

Thus, *in vitro* experiments further strengthen the hypothesis that Prep1 is able to favour neuronal cell viability and functionality by controlling TrkB-mediated neurotrophic signalling pathway. To our best knowledge, no previous evidences have underlined association between Prep1 (or other TALE family members) and adult neuronal cell responsiveness to TrkB-mediated neurotrophic stimuli, and how this association might impact on olfactory anatomical features and animal behaviour. Future *in vivo* and *in vitro* studies will be necessary to verify whether Prep1-mediated improving of TrkB signalling is able to increase olfactory neurons responsiveness to BDNF, and to clarify the molecular mechanisms by which Prep1 promote TrkB expression. Biocomputational analysis of TrkB gene promoter with MatInspector® software (www.genomatix.de/onlinehelp/helpmatinspector/matinspectorhelp.html), indeed, suggests several *consensus* sequences for Prep1 factor, as well as for its main co-factor, Pbx1, which could be verified by Chromatin Immunoprecipitation (ChIp) Assay or by ChIp-Seq Assay.

Although further investigations are needed for conclusion to be drawn, results of my study give a first evidence on the role of the homeobox *prep1* gene in regulating olfactory structural and functional integrity, potentially due to an impaired responsiveness of this CNS region to TrkB-dependent neurotrophic stimulation. The most prominent finding has been the morpho-functional defects observed in olfactory system of Prep1 deficient mice, which can have a profound impact on animal behaviour, as well as in control of peripheral organs activity, since olfactory perceptions define a series of neuroendocrine signals which regulate growth, reproduction and general metabolic homeostasis. Olfaction, indeed, represents a major sensory modality in regulation of food consumption and peripheral metabolism, and, in turn, body nutritional status is able to modulate olfactory detection ability (Al Koborssy D *et al.*, 2014; Aimé P *et al.*, 2014). Thus, in agreement with recent reports (Thiebaud N *et al*., 2014; Takase K *et al*., 2016), it is possible to hypothesize that impaired olfactory perception featured by Prep1 hypomorphic mice might mimic satiety status which, thereby, favour peripheral nutrient utilization, as observed in our previous studies.

In addition, dealing with recent interests in identifying the developmental origin of impaired neurological phenotypes observed in disorders like Parkinson's or Huntington's, this study could also provide a potential genetic marker which, in the near future, could be rationally associated to specific neurological features (olfaction and locomotor impairments) observed in patients and could represent also a promising target.

6. REFERENCES

Agoston Z, Heine P, Brill MS, Grebbin BM, Hau AC, Kallenborn-Gerhardt W, Schramm J, Götz M, Schulte D. Meis2 is a Pax6 co-factor in neurogenesis and dopaminergic periglomerular fate specification in the adult olfactory bulb. Development. 2014;141:28-38.

Aimé P, Palouzier-Paulignan B, Salem R, Al Koborssy D, Garcia S, Duchamp C, Romestaing C, Julliard AK. Modulation of olfactory sensitivity and glucose-sensing by the feeding state in obese Zucker rats. Front Behav Neurosci. 2014; 8:326.

Al Koborssy D, Palouzier-Paulignan B, Salem R, Thevenet M, Romestaing C, Julliard AK. Cellular and molecular cues of glucose sensing in the rat olfactory bulb. Front Neurosci. 2014; 8:333.

Alexander T, Nolte C, Krumlauf R. Hox genes and segmentation of the hindbrain and axial skeleton. Annu Rev Cell Dev Biol. 2009; 25:431-456.

Arruda D, Publio R, Roque AC. The periglomerular cell of the olfactory bulb and its role in controlling mitral cell spiking: a computational model. PLoS One. 2013; 8:e56148.

Arsenijevic Y, Weiss S. Insulin-like growth factor-I is a differentiation factor for postmitotic CNS stem cell-derived neuronal precursors: distinct actions from those of brain-derived neurotrophic factor. J Neurosci. 1998; 18:2118-2128.

Azcoitia V, Aracil M, Carlos-Martinez A and Torres M. The homeodomain protein Meis1 is essential for definitive hematopoiesis and vascular patterning in the mouse embryo. Dev Biol 2005; 280: 307–320.

Barber BA, Liyanage VR, Zachariah RM, Olson CO, Bailey MA, Rastegar M. Dynamic expression of MEIS1 homeoprotein in E14.5 forebrain and differentiated forebrain-derived neural stem cells. Ann Anat. 2013; 195: 431-440.

Bartkowska K, Turlejski K, Djavadian RL. Neurotrophins and their receptors in early development of the mammalian nervous system. Acta Neurobiol Exp (Wars). 2010; 70:454-467.

Bath KG, Lee FS. Neurotrophic factor control of adult SVZ neurogenesis. Dev Neurobiol. 2010; 70:339-349.

Bath KG, Akins MR, Lee FS. BDNF control of adult SVZ neurogenesis. Dev Psychobiol. 2012;54:578-589.

Bol SM, Booiman T, van Manen D, Bunnik EM, van Sighem AI, Sieberer M, Boeser-Nunnink B, de Wolf F, Schuitemaker H, Portegies P, Kootstra NA, van 't Wout AB. Single nucleotide polymorphism in gene encoding transcription factor Prep1 is associated with HIV-1-associated dementia. PLoS One. 2012; 7:e30990.

Bothwell M. Recent advances in understanding neurotrophin signaling. F1000 Res. 2016;5. pii: F1000 Faculty Rev-1885.

Chiaramello S, Dalmasso G, Bezin L, Marcel D, Jourdan F, Peretto P, Fasolo A, De Marchis S. BDNF/TrkB interaction regulates migration of SVZ

precursor cells via PI3-K and MAP-K signalling pathways. Eur J Neurosci. 2007; 26:1780-1790.

Choe SK, Vlachakis N, Sagerström CG. Meis family proteins are required for hindbrain development in the zebrafish. Development. 2002; 129: 585-595.

Deflorian G, Tiso N, Ferretti E, Meyer D, Blasi F, Bortolussi M, Argenton F. Prep1.1 has essential genetic functions in hindbrain development and cranial neural crest cell differentiation. Development. 2004; 131: 613-627.

DiMartino JF, Selleri L, Traver D, Firpo M, Rhee J, Warnke R, O'Gorman S, Weissman IL and Cleary ML. The Hox cofactor and protoncogene Pbx1 is required for maintenance of definitive hematopoiesis in the fetal liver. Blood 2001; 98: 618–626.

Erickson T, Scholpp S, Brand M, Moens CB, Waskiewicz AJ. Pbx proteins cooperate with Engrailed to pattern the midbrain-hindbrain and diencephalic-mesencephalic boundaries. Dev Biol. 2007; 301: 504-517..

Fernandez-Diaz LC, Laurent A, Girasoli S, Turco M, Longobardi E, Iotti G, Jenkins NA, Fiorenza MT, Copeland NG and Blasi F. The absence of Prep1 causes p53-dependent apoptosis of mouse pluripotent epiblast cells. Development 2010; 137: 3393-3403.

Ferretti E, Marshall H, Pöpperl H, Maconochie M, Krumlauf R, Blasi F. Segmental expression of Hoxb2 in r4 requires two separate sites that integrate cooperative interactions between Prep1, Pbx and Hox proteins. Development. 2000; 127:155-166.

Ferretti E, Cambronero F, Tümpel S, Longobardi E, Wiedemann LM, Blasi F, Krumlauf R. Hoxb1 enhancer and control of rhombomere 4 expression: complex interplay between PREP1-PBX1-HOXB1 binding sites. Mol Cell Biol. 2005; 25:8541-8552.

Ferretti E, Villaescusa JC, Di Rosa P, Fernandez-Diaz LC, Longobardi E, Mazzieri R, Miccio A, Micali N, Selleri L, Ferrari G and Blasi F. Hypomorphic mutation of the TALE gene Prep1 (pKnox1) causes a major reduction of Pbx and Meis proteins and a pleiotropic embryonic phenotype. Mol Cell Biol 2006; 26: 5650-5662.

Gascon E, Vutskits L, Zhang H, Barral-Moran MJ, Kiss PJ, Mas C, Kiss JZ. Sequential activation of p75 and TrkB is involved in dendritic development of subventricular zone-derived neuronal progenitors in vitro. Eur J Neurosci. 2005;21:69-80

Gheusi G, Cremer H, McLean H, Chazal G, Vincent JD, Lledo PM. Importance of newly generated neurons in the adult olfactory bulb for odor discrimination. Proc Natl Acad Sci U S A. 2000;97:1823-1828.

Gilbert SF. Developmental Biology. 6th edition. Sunderland (MA): Sinauer Associates; 2000. Differentiation of the Neural Tube. Available from: https://www.ncbi.nlm.nih.gov/books/NBK10034/

Glover JC. Correlated patterns of neuron differentiation and Hox gene expression in the hindbrain: a comparative analysis. Brain Res Bull. 2001;55:683-693.

Guimaraes IM, Carvalho TG, Ferguson SS, Pereira GS, Ribeiro FM. The metabotropic glutamate receptor 5 role on motor behavior involves specific neural substrates. Mol Brain. 2015;8:24.

Hagan CE, Bolon B, Keene CD. Nervous System (chapter 20); "Comparative Anatomy and Histology" Edited by: Treuting PM, Dintzis S, Liggitt D and Frevert CW. Elsevier Inc. 2012, ISBN: 978-0-12-381361-9

Hagg T. Molecular regulation of adult CNS neurogenesis: an integrated view. Trends Neurosci. 2005; 28:589-595.

Hisa T, Spence SE, Rachel RA, Fujita M, Nakamura T, Ward JM, Devor-Henneman DE, Saiki Y, Kutsuna H, Tessarollo L, Jenkins NA and Copeland NG. Hematopoietic, angiogenic and eye defects in Meis1 mutant animals. EMBO J 2004; 23: 450–459.

Holland PW, Takahashi T. The evolution of homeobox genes: Implications for the study of brain development. Brain Res Bull. 2005;66:484-490.

Huang EJ, Reichardt LF. Neurotrophins: roles in neuronal development and function. Annu Rev Neurosci. 2001; 24:677-6736.

Hrycaj SM, Wellik DM. Hox genes and evolution. F1000Res. 2016;5. pii: F1000 Faculty Rev-859.

Imai T. Construction of functional neuronal circuitry in the olfactory bulb. Semin Cell Dev Biol. 2014;35:180-188.

Jacobs Y, Schnabel CA, Cleary ML Trimeric association of Hox and TALE homeodomain proteins mediates Hoxb2 hindbrain enhancer activity. Mol Cell Biol. 1999; 19:5134-5142.

Li H, Zhang P, Fu G, Li J, Liu H, Li Z. Alterations in tyrosine kinase receptor (Trk) expression induced by insulin-like growth factor-1 in cultured dorsal root ganglion neurons. Brain Res Bull. 2013; 90:25-34.

Longobardi E, Penkov D, Mateos D, De Florian G, Torres M, Blasi F. Biochemistry of the tale transcription factors PREP, MEIS, and PBX in vertebrates. Dev Dyn. 2014;243:59-75.

Machon O, Masek J, Machonova O, Krauss S, Kozmik Z. Meis2 is essential for cranial and cardiac neural crest development. BMC Dev Biol. 2015; 15:40.

Moens CB, Selleri L. Hox cofactors in vertebrate development. Dev Biol 2006; 291: 193–206.

Mori K, Nagao H, Yoshihara Y (1999) The olfactory bulb: coding and processing of odor molecule information. Science 286: 711–715.

Mouradian LE, Scott JW. Cytochrome oxidase staining marks dendritic zones of the rat olfactory bulb external plexiform layer. J Comp Neurol. 1988;271:507-518.

Nieto-Estévez V, Defterali Ç, Vicario-Abejón C. IGF-I: A Key Growth Factor that Regulates Neurogenesis and Synaptogenesis from Embryonic to Adult Stages of the Brain. Front Neurosci. 2016;10:52.

Oriente F, Fernandez Diaz LC, Miele C, Iovino S, Mori S, Diaz VM, Troncone G, Cassese A, Formisano P, Blasi F and Beguinot F. Prep1 deficiency induces protection from diabetes and increased insulin sensitivity through a p160-mediated mechanism. Mol Cell Biol 2008; 28: 5634-5645.

Oriente F, Iovino S, Cabaro S, Cassese A, Longobardi E, Miele C, Ungaro P, Formisano P, Blasi F and Beguinot F. Prep1 controls insulin glucoregulatory function in liver by transcriptional targeting of SHP1 tyrosine phosphatase. Diabetes 2011; 60: 138-147.

Oriente F, Cabaro S, Liotti A, Longo M, Parrillo L, Pagano TB, Raciti GA, Penkov D, Paciello O, Miele C, Formisano P, Blasi F, Beguinot F. PREP1 deficiency downregulates hepatic lipogenesis and attenuates steatohepatitis in mice. Diabetologia. 2013; 56: 2713-2722.

Parrilla M, Chang I, Degl'Innocenti A, Omura M. Expression of homeobox genes in the mouse olfactory epithelium. J Comp Neurol. 2016;524:2713-2739.

Parnavelas JG.The origin and migration of cortical neurones: new vistas. Trends Neurosci. 2000; 23:126-131.

Penkov D, Di Rosa P, Fernandez Diaz L, Basso V, Ferretti E, Grassi F, Mondino A and Blasi F. Involvement of Prep1 in the alpha beta T-cell receptor T-lymphocytic potential of hematopoietic precursor. Mol Cell Biol 2005; 25: 10768-10781.

Pereira PL, Magnol L, Sahún I, Brault V, Duchon A, Prandini P, Gruart A, Bizot JC, Chadefaux-Vekemans B, Deutsch S, Trovero F, Delgado-García JM, Antonarakis SE, Dierssen M, Herault Y. A new mouse model for the trisomy

of the Abcg1-U2af1 region reveals the complexity of the combinatorial genetic code of down syndrome. Hum Mol Genet. 2009; 18:4756-4769.

Rave-Harel N, Givens ML, Nelson SB, Duong HA, Coss D, Clark ME, Hall SB, Kamps MP, Mellon PL. TALE homeodomain proteins regulate gonadotropin-releasing hormone gene expression independently and via interactions with Oct-1. J Biol Chem. 2004; 279:30287-30297

Redmond L, Hockfield S, Morabito MA. The divergent homeobox gene PBX1 is expressed in the postnatal subventricular zone and interneurons of the olfactory bulb. J Neurosci. 1996;16:2972-2982.

Reichardt LF. Neurotrophin-regulated signalling pathways. Philos Trans R Soc Lond B Biol Sci. 2006; 361:1545-1564.

Rice D, Barone S Jr. Critical periods of vulnerability for the developing nervous system: evidence from humans and animal models. Environ Health Perspect. 2000; 108 Suppl 3:511-533.

Rijli FM, Gavalas A, Chambon P. Segmentation and specification in the branchial region of the head: the role of the Hox selector genes. Int J Dev Biol. 1998; 42:393-401.

Sánchez-Font MF, Bosch-Comas A, Gonzàlez-Duarte R, Marfany G. Overexpression of FABP7 in Down syndrome fetal brains is associated with PKNOX1 gene-dosage imbalance. Nucleic Acids Res. 2003; 31: 2769-2777.

Schulte D, Frank D. TALE transcription factors during early development of the vertebrate brain and eye. Dev Dyn. 201; 243:99-116.

Sgadò P, Ferretti E, Grbec D, Bozzi Y, Simon HH. 2012. The atypical homeoprotein Pbx1a participates in the axonal pathfinding of mesencephalic dopaminergic neurons. Neural Dev 7:24.

Shim S, Kim Y, Shin J, Kim J, Park S. Regulation of EphA8 gene expression by TALE homeobox transcription factors during development of the mesencephalon. Mol Cell Biol. 2007; 27:1614-1630.

Stoleru B, Popescu AM, Tache DE, Neamtu OM, Emami G, Tataranu LG, Buteica AS, Dricu, Purcarua SO.Tropomyosin-Receptor-Kinases Signaling in the Nervous System Maedica (Buchar). 2013; 8: 43–48.

Takase K, Tsuneoka Y, Oda S, Kuroda M, Funato H. High-fat diet feeding alters olfactory-, social-, and reward-related behaviors of mice independent of obesity. Obesity (Silver Spring). 2016; 24:886-894.

Taylor TN, Greene JG, Miller GW. Behavioral phenotyping of mouse models of Parkinson's disease. Behav Brain Res. 2010; 211:1-10

Thiebaud N, Johnson MC, Butler JL1, Bell GA, Ferguson KL, Fadool AR, Fadool JC, Gale AM, Gale DS, Fadool DA. Hyperlipidemic diet causes loss of olfactory sensory neurons, reduces olfactory discrimination, and disrupts odor-reversal learning. J Neurosci. 2014; 34:6970-6984.

Toresson H, Parmar M, Campbell K. Expression of Meis and Pbx genes and their protein products in the developing telencephalon: implications for regional differentiation. Mech Dev. 2000; 94:183-187.

Trainor PA, Manzanares M, Krumlauf R. Mouse Brain Development. Andre M. Goffinet, Pasko Rakic (eds). Genetic Interaction During Hindbrain Segmentation in the Mouse Embryo. Springer-Verlag 2000 ISBN 978-3-642-53684-7 doi 10.1007/978-3-540-48002-0

Tanja Vogel (2013). Insulin/IGF-Signalling in Embryonic and Adult Neural Proliferation and Differentiation in the Mammalian Central Nervous System, Trends in Cell Signaling Pathways in Neuronal Fate Decision, Dr Sabine Wislet-Gendebien (Ed.), InTech 2013, DOI: 10.5772/54946.

Wright EK Jr, Page SH, Barber SA, Clements JE. Prep1/Pbx2 complexes regulate CCL2 expression through the -2578 guanine polymorphism. Genes Immun. 2008; 9: 419-430.

Whitlock KE. The loss of scents: do defects in olfactory sensory neuron development underlie human disease? Birth Defects Res C Embryo Today. 2015; 105:114-125.

Yuan TF. BDNF signaling during olfactory bulb neurogenesis. J Neurosci. 2008;28:5139-5140.